Entanglement entropy and conformal field theory

2009 J. Phys. A: Math. Theor. 42 504005

(http://iopscience.iop.org/1751-8121/42/50/504005)

IOP PUBLISHING JOURNAL OF PHYSICS A: MATHEMATICAL AND THEORETICAL

J. Phys. A: Math. Theor. **42** (2009) 504005 (36pp) doi:10.1088/1751-8113/42/50/504005

Entanglement entropy and conformal field theory

Pasquale Calabrese[1] **and John Cardy**[2,3]

[1] Dipartimento di Fisica dell'Università di Pisa and INFN, Pisa, Italy
[2] Oxford University, Rudolf Peierls Centre for Theoretical Physics, 1 Keble Road, Oxford, OX1 3NP, UK
[3] All Souls College, Oxford, UK

E-mail: calabres@df.unipi.it

Received 28 May 2009, in final form 15 September 2009
Published 2 December 2009
Online at stacks.iop.org/JPhysA/42/504005

Abstract
We review the conformal field theory approach to entanglement entropy in 1+1 dimensions. We show how to apply these methods to the calculation of the entanglement entropy of a single interval, and the generalization to different situations such as finite size, systems with boundaries and the case of several disjoint intervals. We discuss the behaviour away from the critical point and the spectrum of the reduced density matrix. Quantum quenches, as paradigms of non-equilibrium situations, are also considered.

PACS numbers: 64.70.Tg, 03.67.Mn, 75.10.Pq

1. Introduction

Entanglement is one of the most fundamental and fascinating features of quantum mechanics, yet in some ways the most mysterious: performing a local measure may instantaneously affect the outcome of local measurements far away. This phenomenon has been the basis for the development of such new branches of research as quantum information and communication. A very recent and rich field of research concerns the understanding of the role of entanglement in many-body systems.

Besides its own fundamental theoretical interest, a principal reason for the success of the entanglement entropy as an entanglement measure in extended quantum systems is surely its universal scaling at one-dimensional (1D) conformal critical points. The following equation [1–3]

$$S_A = \frac{c}{3} \ln \frac{\ell}{a} + c_1' \tag{1}$$

has become one of the most ubiquitous formulae in the literature over the last 5 years, appearing in fields as apparently unrelated as quantum information, condensed matter and high energy physics. The reasons for this prominence are clear: it is a single quantity, easily measurable in numerical simulations, that at the same time gives the location of the critical point and one

of its most important universal signatures, the *central charge c* of the underlying conformal field theory (CFT).

The aim of this paper is to give a self-contained presentation of most of the results for the entanglement entropy that can be obtained by means of CFT. Some other important features of the entanglement in extended quantum systems will only be considered on passing. For a comprehensive treatment of these aspects we refer the reader to the other review in this special issue [4] and to the already existing ones [5, 6].

The plan of this paper is as follows. In section 2 we review the CFT (and more generally quantum field theory) approach to entanglement entropy based on the replica trick, the mapping to the partition function on Riemann surfaces and the introduction of twist fields. In section 3 we apply these methods to the calculation of the entanglement entropy of a single interval, showing in particular how to obtain equation (1), and generalizing it to several different situations, like finite size, finite temperature, systems with boundaries and defects. In section 4 we consider the case of several disjoint intervals, with particular attention to the case of two intervals, where several results are now available. In section 5 we consider massive perturbations to the conformal behaviour in the regime when the mass is small and the systems still retain signatures of the close conformal critical point. In section 6 we derive the consequences of the conformal scaling for the full spectrum of the reduced density matrix. In section 7 we discuss the CFT approach to non-equilibrium situations known as quantum quenches. Finally in section 8 we report on an interesting proposal of Klich and Levitov [7] to measure the entanglement entropy in real experiments.

2. Entanglement, replicas, Riemann surfaces, twist fields and all that

2.1. Basic definitions

Let ρ be the density matrix of a system, which we take to be in the pure quantum state $|\Psi\rangle$, so that $\rho = |\Psi\rangle\langle\Psi|$. Let the Hilbert space be written as a direct product $\mathcal{H} = \mathcal{H}_A \otimes \mathcal{H}_B$. A's reduced density matrix is $\rho_A = \mathrm{Tr}_B \rho$. The entanglement entropy is the corresponding von Neumann entropy

$$S_A = -\mathrm{Tr}\rho_A \ln \rho_A, \tag{2}$$

and analogously for S_B. When ρ corresponds to a pure quantum state $S_A = S_B$. For future use, we also define the Rényi entropies

$$S_A^{(n)} = \frac{1}{1-n} \ln \mathrm{Tr}\rho_A^n, \tag{3}$$

that are also characterized by $S_A^{(n)} = S_B^{(n)}$ whenever ρ corresponds to a pure quantum state. From these definitions $S_A = \lim_{n\to 1} S_A^{(n)}$.

When a system is in a mixed state the entanglement entropy is no longer a good measure of entanglement since it clearly mixes quantum and classical correlations (e.g. in a high temperature mixed state, it must reproduce the extensive result for the thermal entropy that has nothing to do with entanglement). This is also evident from the fact that S_A is no longer equal to S_B. A quantity that is easily constructed from the knowledge of S_A and S_B is the so-called mutual information, defined from the Rényi entropy as

$$I_{A:B}^{(n)} = S_A^{(n)} + S_B^{(n)} - S_{A\cup B}^{(n)}, \tag{4}$$

that is by definition symmetric in A and B. $I_{A:B}^{(n)}$ does not have all the correct properties to be an entanglement measure (see the review by Amico and Fazio in this special issue [8] for a discussion of various entanglement measures), but it has the fundamental property of satisfying the area law [6, 9], even at finite temperature [10].

2.2. A replica approach

When dealing with a statistical model with a finite number of degrees of freedom, the most direct way to obtain the entanglement entropy is to construct the reduced density matrix (or at least its eigenvalues λ_i as in density-matrix renormalization group (DMRG)) exactly or numerically and then, by brute force or by analytic methods, calculate the sum $S_A = -\sum \lambda_i \ln \lambda_i$. Several examples of how this can be worked out, even analytically, for the simplest models are reported in other reviews in this special issue. However, calculating the full reduced density matrix for a generic interacting quantum field theory remains a daunting challenge from an operational point of view, and so here we will take a different route, following our previous papers [3, 11–13]. The approach is reminiscent of the 'replica trick' in disordered systems and was present in an embryonic form also in the early paper by Holzhey *et al* [1]. Let us start by considering a lattice model. The eigenvalues of the reduced density matrix λ_i lie in the interval [0, 1] and $\sum \lambda_i = 1$. Thus, for any $n \geqslant 1$ (even not integer), the sum $\mathrm{Tr}\,\rho_A^n = \sum_i \lambda_i^n$ is absolutely convergent and therefore analytic for all $\mathrm{Re}\, n > 1$. The derivative wrt n therefore also exists and is analytic in the region. Moreover, if the entropy $S_A = -\sum_i \lambda_i \log \lambda_i$ is finite, the limit as $n \to 1^+$ of the first derivative converges to this value. Thus, if we are able to calculate $\mathrm{Tr}\,\rho_A^n$ for any $n \geqslant 1$ we have the entanglement entropy as

$$S_A = -\lim_{n\to 1} \frac{\partial}{\partial n} \mathrm{Tr}\,\rho_A^n = \lim_{n\to 1} S_A^{(n)}. \tag{5}$$

However, calculating $\mathrm{Tr}\,\rho_A^n$ for a generic real n in a quantum field theory is still a hopeless task. And here the 'replica trick' enters: we compute $\mathrm{Tr}\,\rho_A^n$ only for a positive integral n and then analytically continue it to a general complex value. We will see that the calculation of $\mathrm{Tr}\,\rho_A^n$ reduces to that of a partition function on a complicated Riemann surface (or equivalently to the correlation function of specific *twist fields*) that is analytically achievable in a quantum field theory. The problem is then moved to the existence and the uniqueness of a proper analytic continuation to extract the entanglement entropy (as in any approach based on replicas). In some cases this is straightforward, in others difficult and in several others beyond our present understanding.

2.3. Path integral formulation and Riemann surfaces

To begin with a well-defined problem, let us consider a lattice quantum theory in one-space and one-time dimensions (the generalization to higher spatial dimensions is straightforward). The lattice sites are labelled by a discrete variable x and the lattice spacing is a. The domain of x can be finite, i.e. some interval of length L, semi-infinite, or infinite. Time is continuous. A complete set of local commuting observables will be denoted by $\{\hat{\phi}_x\}$, and their eigenvalues and corresponding eigenstates by $\{\phi_x\}$ and $|\{\phi_x\}\rangle$, respectively. (For a bosonic lattice field theory, these will be the fundamental bosonic fields of the theory; for a spin model some particular component of the local spin.) The states $\otimes_x |\{\phi_x\}\rangle = |\prod_x \{\phi_x\}\rangle$ form a basis. The dynamics of the theory is described by the Hamiltonian H. The elements of the density matrix ρ in a thermal state at inverse temperature β are

$$\rho(\{\phi_x\}|\{\phi'_{x'}\}) \equiv \left\langle \prod_x \{\phi_x\}|\rho|\prod_{x'} \{\phi'_{x'}\} \right\rangle = Z(\beta)^{-1} \left\langle \prod_x \{\phi_x\}|\, \mathrm{e}^{-\beta H}|\prod_{x'} \{\phi_{x'}\} \right\rangle, \tag{6}$$

where $Z(\beta) = \mathrm{Tr}\,\mathrm{e}^{-\beta H}$ is the partition function. This may be written as a path integral on the imaginary time interval $(0, \beta)$:

$$\rho(\{\phi_x\}|\{\phi'_{x'}\}) = Z^{-1} \int [\mathrm{d}\phi(y,\tau)] \prod_{x'} \delta(\phi(y,0) - \phi'_{x'}) \prod_x \delta(\phi(y,\beta) - \phi_x)\, \mathrm{e}^{-S_E}, \tag{7}$$

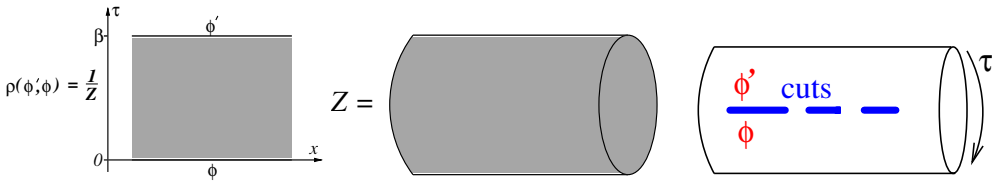

Figure 1. From density matrix to reduced density matrix. Left: path integral representation of $\rho(\phi|\phi')$. Centre: the partition function Z is obtained by sewing together the edges along $\tau = 0$ and $\tau = \beta$ to form a cylinder of circumference β. Right: the reduced density matrix ρ_A is obtained by sewing together only those points x which are not in A.

where the Euclidean action is $S_E = \int_0^\beta L\,\mathrm{d}\tau$, with L the Euclidean Lagrangian. This is illustrated in the left panel of figure 1. Here the rows and columns of the reduced density matrix are labelled by the values of the fields at $\tau = 0, \beta$.

The normalization factor Z is the partition function, and ensures that $\mathrm{Tr}\rho = 1$. It is found by setting $\{\phi_x\} = \{\phi'_x\}$ and integrating over these variables. In the path integral, this has the effect of sewing together the edges along $\tau = 0$ and $\tau = \beta$ to form a cylinder of circumference β as depicted in the centre of figure 1.

Now let A be a subsystem consisting of the points x in the disjoint intervals $(u_1, v_1), \ldots, (u_N, v_N)$. An expression for the reduced density matrix ρ_A is obtained from (7) by sewing together only those points x which are not in A. This has the effect of leaving open cuts, one for each interval (u_j, v_j), along the line $\tau = 0$ as in the right panel of figure 1.

We may then compute $\mathrm{Tr}\,\rho_A^n$, for any positive integer n, by making n copies of the above, labelled by an integer j with $1 \leqslant j \leqslant n$, and sewing them together cyclically along the cuts so that $\phi_j(x, \tau = \beta^-) = \phi_{j+1}(x, \tau = 0^+)$ and $\phi_n(x, \tau = \beta^-) = \phi_1(x, \tau = 0^+)$ for all $x \in A$. This defines an n-sheeted structure depicted for $n = 3$ and in the case when A is a single interval in figure 2. The partition function on this surface will be denoted by $Z_n(A)$ and so

$$\mathrm{Tr}\,\rho_A^n = \frac{Z_n(A)}{Z^n}. \tag{8}$$

When the right-hand side of the above equation has a unique analytic continuation to $\mathrm{Re}\,n > 1$, its first derivative at $n = 1$ gives the required entropy

$$S_A = -\lim_{n\to 1} \frac{\partial}{\partial n} \frac{Z_n(A)}{Z^n}. \tag{9}$$

So far, everything has been for a discrete space domain. We now discuss the continuum limit, in which $a \to 0$ keeping all other lengths fixed. The points x then assume real values, and the path integral is over fields $\phi(x, \tau)$ on an *n-sheeted Riemann surface*, with branch points at u_j and v_j. In this limit, S_E is supposed to go over into the Euclidean action for a quantum field theory. We indicate these n-sheeted surfaces with $\mathcal{R}_{n,N}$ and they are fully defined by the $2N$ branch points u_j and v_j. Whenever the value of n and N is not important, we will simply indicate the surface with $\mathcal{R}$.

In the following, we will focus our attention on the case when the quantum field theory is Lorentz invariant, since the full power of relativistic field theory can then be brought to bear. The behaviour of partition functions in this limit has been well studied. In two dimensions, the logarithm of a general partition function Z in a domain with total area $\mathcal{A}$ and with boundaries

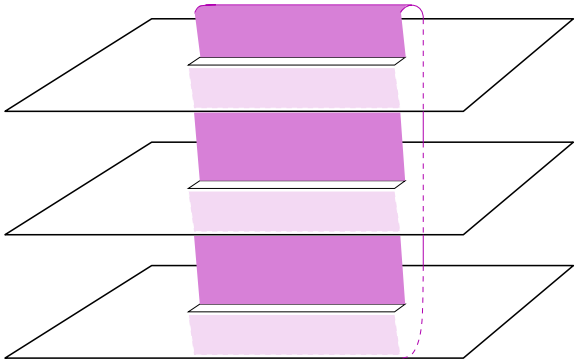

Figure 2. A representation of the Riemann surface $\mathcal{R}_{3,1}$. Reprinted with permission from [12].

of total length $\mathcal{L}$ behaves as

$$\log Z = f_1 \mathcal{A} a^{-2} + f_2 \mathcal{L} a^{-1} + \cdots \tag{10}$$

where f_1 and f_2 are the non-universal bulk and boundary-free energies. Note, however, that these leading terms *cancel* in the ratio of partition functions in (8).

In a conformal field theory, as was argued by Cardy and Peschel [14], there are also *universal* terms proportional to $\log a$. These arise from the points of the non-zero curvature of the manifold and its boundary. In our case, these are conical singularities at the branch points. In fact, it is precisely these logarithmic terms which give rise to the non-trivial dependence of the final result for the entropy on the short-distance cut-off a. For the moment let us simply note that, in order to achieve a finite limit as $a \to 0$, the right-hand side of (8) should be multiplied by some renormalization constant $\mathcal{Z}(A, n)$.

2.4. From replicated world-sheet to replicated target-space: twist fields

In the simplest instances it is possible to directly calculate the partition function on a n-sheeted Riemann surface, but in most of the cases this is very difficult. However, the surface we are dealing with has curvature zero everywhere except at a finite number of points (i.e. the boundaries between A and B u_j, v_j above). Since the Lagrangian density does not depend explicitly on the Riemann surface $\mathcal{R}$ as a consequence of its locality, it is expected that the partition function can be expressed as an object calculated from a model on the complex plane $\mathbf{C}$, where the structure of the Riemann surface is implemented through appropriate boundary conditions around the points with non-zero curvature. Consider for instance the simple Riemann surface $\mathcal{R}_{n,1}$ needed for the calculation of the entanglement entropy of a single interval $[u_1, v_1]$, made of n sheets sequentially joined to each other on the segment $x \in [u_1, v_1]$, $\tau = 0$. We expect that the associated partition function in a theory defined on the complex plane $z = x + \mathrm{i}\tau$ can be written in terms of certain 'fields' at $z = v_1$ and $z = u_1$.

The partition function (here $\mathcal{L}[\varphi](x, \tau)$ is the local Lagrangian *density*)

$$Z_{\mathcal{R}} = \int [\mathrm{d}\varphi]_{\mathcal{R}} \exp\left[- \int_{\mathcal{R}} \mathrm{d}x \, \mathrm{d}\tau \mathcal{L}[\varphi](x, \tau) \right], \tag{11}$$

essentially defines these fields, i.e. it gives their correlation functions, up to a normalization independent of their positions. However, in the model on the complex plane, this definition makes them non-local (see for a complete discussion [12]). Locality is at the basis of most of the results in field theory, so it is important to recover it.

The solution to the problem consists in moving the complicated topology of the world sheet $\mathcal{R}$ (i.e. the space where the coordinates x, τ live) to the target space (i.e. the space where the fields live). Let us consider a model formed by n independent copies of the original model. (Note that n is the number of Riemann sheets necessary to describe the Riemann surface by the coordinates on the plane.) The partition function (11) can be re-written as the path integral on the complex plane

$$Z_{\mathcal{R}} = \int_{\mathcal{C}_{u_1,v_1}} [\mathrm{d}\varphi_1 \cdots \mathrm{d}\varphi_n] \exp\left[- \int_{\mathbf{C}} \mathrm{d}x\, \mathrm{d}\tau\, (\mathcal{L}[\varphi_1](x,\tau) + \cdots + \mathcal{L}[\varphi_n](x,\tau)) \right] \tag{12}$$

where with $\int_{\mathcal{C}_{u_1,v_1}}$ we indicated the *restricted* path integral with conditions

$$\varphi_i(x, 0^+) = \varphi_{i+1}(x, 0^-), \qquad x \in [u_1, v_1], \quad i = 1, \ldots, n \tag{13}$$

where we identify $n + i \equiv i$. The Lagrangian density of the multi-copy model is

$$\mathcal{L}^{(n)}[\varphi_1, \ldots, \varphi_n](x,\tau) = \mathcal{L}[\varphi_1](x,\tau) + \cdots + \mathcal{L}[\varphi_n](x,\tau)$$

so that the energy density is the sum of the energy densities of the n individual copies. Hence the expression (12) does indeed define local fields at $(u_1, 0)$ and $(v_1, 0)$ in the multi-copy model [12].

The local fields defined in (12) are examples of 'twist fields'. Twist fields exist in a quantum field theory whenever there is a global internal symmetry σ (a symmetry that acts the same way everywhere in space, and that does not change the positions of fields): $\int \mathrm{d}x\, \mathrm{d}\tau\, \mathcal{L}[\sigma\varphi](x,\tau) = \int \mathrm{d}x\, \mathrm{d}\tau\, \mathcal{L}[\varphi](x,\tau)$. In the model with Lagrangian $\mathcal{L}^{(n)}$, there is a symmetry under exchange of the copies. The twist fields defined by (12), which have been called *branch-point twist fields* [12], are twist fields associated with the two opposite cyclic permutation symmetries $i \mapsto i + 1$ and $i + 1 \mapsto i$ ($i = 1, \ldots, n,\ n + 1 \equiv 1$). We can denote them simply by $\mathcal{T}_n$ and $\tilde{\mathcal{T}}_n$, respectively:

$$\mathcal{T}_n \equiv \mathcal{T}_\sigma, \quad \sigma : i \mapsto i + 1 \mod n, \tag{14}$$

$$\tilde{\mathcal{T}}_n \equiv \mathcal{T}_{\sigma^{-1}}, \quad \sigma^{-1} : i + 1 \mapsto i \mod n. \tag{15}$$

Note that $\tilde{\mathcal{T}}_n$ can be identified with $\mathcal{T}_{-n}$ (and in fact they were called Φ_n and Φ_{-n} in [3]).

For the n-sheeted Riemann surface along the set A made of N disjoint intervals $[u_j, v_j]$ we then have

$$Z_{\mathcal{R}_{n,N}} \propto \langle \mathcal{T}_n(u_1,0)\tilde{\mathcal{T}}_n(v_1,0) \cdots \mathcal{T}_n(u_N,0)\tilde{\mathcal{T}}_n(v_N,0)\rangle_{\mathcal{L}^{(n)},\mathbf{C}}. \tag{16}$$

This can be seen by observing that for $x \in [u_j, v_j]$, consecutive copies are connected through $\tau = 0$ due to the presence of $\mathcal{T}_n(v_j, 0)$, whereas for x in B, copies are connected to themselves through $\tau = 0$ because the conditions arising from the definition of $\mathcal{T}_n(u_j, 0)$ and $\tilde{\mathcal{T}}_n(v_j, 0)$ cancel each other. More generally, the identification holds for correlation functions in the model $\mathcal{L}$ on $\mathcal{R}_{n,1}$:

$$\langle \mathrm{O}(x,\tau;\text{sheet } i) \cdots \rangle_{\mathcal{L},\mathcal{R}_{n,1}} = \frac{\langle \mathcal{T}_n(u_1,0)\tilde{\mathcal{T}}_n(v_1,0)\mathrm{O}_i(x,\tau)\cdots\rangle_{\mathcal{L}^{(n)},\mathbf{C}}}{\langle \mathcal{T}_n(u_1,0)\tilde{\mathcal{T}}_n(v_1,0)\rangle_{\mathcal{L}^{(n)},\mathbf{C}}} \tag{17}$$

where O_i is the field in the model $\mathcal{L}^{(n)}$ coming from the ith copy of $\mathcal{L}$, and the ratio properly takes into account all the proportionality constants. The same expression with the products of more twist and anti-twist fields holds in the case of $\mathcal{R}_{N,n}$.

It is also useful to introduce the linear combination of the basic fields

$$\tilde{\varphi}_k \equiv \sum_{j=1}^{n} \mathrm{e}^{2\pi i \frac{k}{n} j} \varphi_j, \qquad k = 0, 1, \ldots, n-1, \tag{18}$$

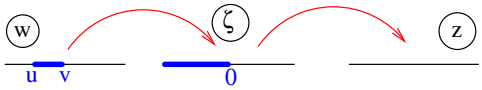

Figure 3. Uniformizing transformation for $\mathcal{R}_{n,1}$. $w \to \zeta = (w-u)/(w-v)$ maps the branch points to $(0,\infty)$. This is uniformized by the mapping $\zeta \to z = \zeta^{1/n}$.

that get multiplied by $\mathrm{e}^{2\pi ik/n}$ on going around the twist operator, i.e. they diagonalize the twist

$$\mathcal{T}_n\tilde{\varphi}_k = \mathrm{e}^{2\pi ik/n}\tilde{\varphi}_k, \qquad \text{and} \qquad \tilde{\mathcal{T}}_n\tilde{\varphi}_k = \mathrm{e}^{-2\pi ik/n}\tilde{\varphi}_k. \tag{19}$$

Note that when the basic field φ_j are real, $\tilde{\varphi}_k^* = \tilde{\varphi}_{n-k}$. When the different values of k decouple, the total partition function is a product of the partition functions for each k. Thus, also the twist fields can be written as products of fields acting only on $\tilde{\varphi}_k$:

$$\mathcal{T}_n = \prod_{k=0}^{n-1}\mathcal{T}_{n,k}, \qquad \tilde{\mathcal{T}}_n = \prod_{k=0}^{n-1}\tilde{\mathcal{T}}_{n,k}, \tag{20}$$

with $\mathcal{T}_{k,n}\tilde{\varphi}_{k'} = \tilde{\varphi}_k$ if $k \neq k'$ and $\mathcal{T}_{k,n}\tilde{\varphi}_k = \mathrm{e}^{2\pi ik/n}\tilde{\varphi}_k$. Thus,

$$Z_{\mathcal{R}} = \prod_{k=0}^{n-1}\langle \mathcal{T}_{k,n}(u_1,0)\tilde{\mathcal{T}}_{k,n}(v_1,0)\cdots\rangle_{\mathcal{L}^{(n)},\mathbf{C}}. \tag{21}$$

This way of proceeding is useful for free theories as in [15–19], when the various k-modes decouple leading to equation (21).

3. Entanglement entropy in conformal field theory: a single interval

Following [3], we first consider the case $N = 1$ and no boundaries, that is the case considered by Holzhey *et al* [1] of a single interval $[u, v]$ of length $\ell \equiv |u - v|$ in an infinitely long 1D quantum system, at zero temperature. The complex coordinate is $w = x + \mathrm{i}\tau$ and $\bar{w} = x - \mathrm{i}\tau$. The conformal mapping $w \to \zeta = (w-u)/(w-v)$ maps the branch points to $(0,\infty)$. This is uniformized by the mapping $\zeta \to z = \zeta^{1/n} = ((w-u)/(w-v))^{1/n}$. This maps the whole of the n-sheeted Riemann surface $\mathcal{R}_{n,1}$ to the z-plane $\mathbf{C}$, see figure 3 for an illustration of this. Now consider the holomorphic component of the stress tensor $T(w)$. This is related to the transformed stress tensor $T(z)$ by [20]

$$T(w) = \left(\frac{\mathrm{d}z}{\mathrm{d}w}\right)^2 T(z) + \frac{c}{12}\{z,w\}, \tag{22}$$

where $\{z,w\} = (z'''z' - \frac{3}{2}z''^2)/z'^2$ is the Schwarzian derivative. In particular, taking the expectation value of this, and using $\langle T(z)\rangle_{\mathbf{C}} = 0$ by translational and rotational invariance, we find

$$\langle T(w)\rangle_{\mathcal{R}_{n,1}} = \frac{c}{12}\{z,w\} = \frac{c(1-n^{-2})}{24}\frac{(v-u)^2}{(w-u)^2(w-v)^2}. \tag{23}$$

From equation (17), this is equal to

$$\frac{\langle \mathcal{T}_n(u,0)\tilde{\mathcal{T}}_n(v,0)T_j(w)\rangle_{\mathcal{L}^{(n)},\mathbf{C}}}{\langle \mathcal{T}_n(u,0)\tilde{\mathcal{T}}_n(v,0)\rangle_{\mathcal{L}^{(n)},\mathbf{C}}},$$

for all j. We can then obtain the correlation function involving the stress-energy tensor of $\mathcal{L}^{(n)}$ by multiplying by n:

$$\frac{\langle \mathcal{T}_n(u,0)\tilde{\mathcal{T}}_n(v,0)T^{(n)}(w)\rangle_{\mathcal{L}^{(n)},\mathbf{C}}}{\langle \mathcal{T}_n(u,0)\mathcal{T}_n(v,0)\rangle_{\mathcal{L}^{(n)},\mathbf{C}}} = \frac{c(n^2-1)}{24n}\frac{(u-v)^2}{(w-u)^2(w-v)^2}.$$

The comparison with the conformal Ward identity [20]

$$\langle \mathcal{T}_n(u,0)\tilde{\mathcal{T}}_n(v,0)T^{(n)}(w)\rangle_{\mathcal{L}^{(n)},\mathbf{C}} = \left(\frac{1}{w-u}\frac{\partial}{\partial u} + \frac{h_{\mathcal{T}_n}}{(w-u)^2} + \frac{1}{w-v}\frac{\partial}{\partial v} + \frac{h_{\tilde{\mathcal{T}}_n}}{(w-v)^2}\right) \times \langle \mathcal{T}_n(u,0)\tilde{\mathcal{T}}_n(v,0)\rangle_{\mathcal{L}^{(n)},\mathbf{C}}, \tag{24}$$

allows us to identify the scaling dimension of the primary fields $\mathcal{T}_n$ and $\tilde{\mathcal{T}}_n$ (they have the same scaling dimension $d_n = \bar{d}_n$) using $\langle \mathcal{T}_n(u,0)\tilde{\mathcal{T}}_n(v,0)\rangle_{\mathcal{L}^{(n)},\mathbf{C}} = |u-v|^{-2d_n}$[4]

$$d_n = \frac{c}{12}\left(n - \frac{1}{n}\right). \tag{25}$$

To our knowledge this scaling dimension was first derived by Knizhnik [21] in a different context.

The above equation determines all the properties under conformal transformations, and we therefore conclude that the renormalized $Z_n(A)/Z^n \propto \mathrm{Tr}\,\rho_A^n$ behaves (apart from a possible overall constant) under scale and conformal transformations identically to the two-point function of a primary operator with dimension d_n. In particular, this means that

$$\mathrm{Tr}\,\rho_A^n = c_n\left(\frac{v-u}{a}\right)^{-c(n-1/n)/6}. \tag{26}$$

The power of a (corresponding to the renormalization constant $\mathcal{Z}$) has been inserted to make the final result dimensionless, as it should be. The constants c_n cannot be determined with this method. However c_1 must be unity. The analytic continuation is straightforward leading to the Rényi and von Neumann entropies

$$S_A^{(n)} = \frac{c}{6}\left(1+\frac{1}{n}\right)\log\frac{\ell}{a} + c_n', \qquad S_A = \frac{c}{3}\log\frac{\ell}{a} + c_1', \tag{27}$$

where we defined the non-universal constant

$$c_n' \equiv \frac{\log c_n}{1-n}. \tag{28}$$

Note that c_1' is minus the derivative of c_n at $n = 1$. Despite their non-universal nature, the constants c_n' are known exactly for few integrable models [12, 22–25].

Under certain conditions, the entanglement entropy can also be expressed in terms of averages over ensembles of random matrices [26] providing a new connection between the universality class of the conformal field theory and random matrix ensembles.

Interestingly, equation (26) describes the asymptotic behaviour for large enough ℓ for any $n > 0$ (and not only for $n \geqslant 1$) at least for the simplest solvable models, where it can be explicitly checked. This is of relevance for the convergence of the algorithms based on matrix product states [27, 28].

3.1. Generalizations: finite temperature or finite size

The fact that $\mathrm{Tr}\,\rho_A^n$ transforms under a general conformal transformation as a two-point function of primary operators $\mathcal{T}$ means that it is simple to compute in other geometries, obtained by a conformal mapping $z \to w = w(z)$, using the formula

$$\langle \mathcal{T}_n(z_1,\bar{z}_1)\tilde{\mathcal{T}}_n(z_2,\bar{z}_2)\rangle = |w'(z_1)w'(z_2)|^{d_n}\langle \mathcal{T}_n(w_1,\bar{w}_1)\tilde{\mathcal{T}}_n(w_2,\bar{w}_2)\rangle. \tag{29}$$

Particularly relevant is the transformation $w \to z = (\beta/2\pi)\log w$ that maps each sheet in the w-plane into an infinitely long cylinder of circumference β. The sheets are now sewn together

[4] We use here d_n instead of Δ_n in [3] to avoid confusion between these scaling dimensions, in fact they are not the same and are related by $d_n = 2n\Delta_n$.

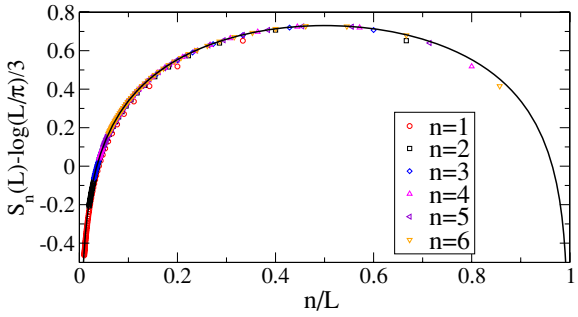

Figure 4. Exact finite size scaling of the entanglement entropy $S_n(L)$ (here $n = \ell$) for the XXZ model at $\Delta = 1/2$ against the CFT prediction $1/3 \log \sin(\pi n/L) + c_1'$ (full line). $c_1' = 0.7305$ has been fixed [33]. Reprinted with permission from [32].

along a branch cut joining the images of the points u and v. By arranging this to lie parallel to the axis of the cylinder, we get an expression for $\mathrm{Tr}\,\rho_A^n$ in a thermal mixed state at finite temperature β^{-1}. After simple algebra, this leads to the result for the entropy [3, 29]

$$S_A = \frac{c}{3} \log \left(\frac{\beta}{\pi a} \sinh \frac{\pi \ell}{\beta} \right) + c_1' = \begin{cases} \dfrac{c}{3} \log \dfrac{\ell}{a} + c_1' & \ell \ll \beta, \\ \dfrac{\pi c}{3\beta} \ell + c_1' & \ell \gg \beta. \end{cases} \tag{30}$$

This simple formula interpolates between the zero-temperature result for $\ell \ll \beta$ and an extensive form in the opposite limit $\ell \gg \beta$. In this limit its density agrees with that of the Gibbs entropy of an isolated system of length ℓ, as obtained from the standard CFT expression [30, 31] $\beta F \sim -(\pi c/6)(\ell/\beta)$ for its free energy. As expected, in the high-temperature limit, the von Neumann entropy reduces to a pure thermal form and the entanglement vanishes.

Alternatively, we may orient the branch cut perpendicular to the axis of the cylinder, which, with the replacement $\beta \to L$, corresponds to the entropy of a subsystem of length ℓ in a finite 1D system of length L, with periodic boundary conditions, in its ground state. This gives

$$\mathrm{Tr}\,\rho_A^n = c_n \left(\frac{L}{\pi a} \sin \frac{\pi \ell}{L} \right)^{-c(n-1/n)/6}, \quad \Rightarrow \quad S_A = \frac{c}{3} \log \left(\frac{L}{\pi a} \sin \frac{\pi \ell}{L} \right) + c_1'. \tag{31}$$

S_A is symmetric under $\ell \to L - \ell$ and it is maximal when $\ell = L/2$. This relation is fundamental in the analysis of numerical data that are mainly done in finite size. It provides an unambiguous way to determine the central charge even from relatively small system sizes. In figure 4 we report the exact calculation of S_A for the XXZ chain at $\Delta = 1/2$ from [32], showing that already small values of ℓ ($\leqslant 6$) it gives the correct asymptotic scaling. We stress that the most powerful aspect in the determination of the central charge via the entanglement entropy is that it does not involve the *a priori* knowledge of the speed of sound, unlike other measures based on the gap or free energy scaling. For this reason, this method has been widely used in recent years.

3.1.1. Finite temperature and finite size. When a finite system is also at finite temperature, we need to consider periodic boundary conditions both on space and imaginary time axes. This results in the calculation of a two-point function of twist operators on a *torus*. As it is well known [34], in this case correlations not only depend on the scaling dimensions, but also on

the full operator content of the theory and the calculations must be done for any universality class. Furthermore, it is not possible to use a uniformizing transformation from the plane because of the non-trivial topology of the torus.

To our knowledge, this calculation has been performed only for the massless Dirac fermion [35]. In this case, it is convenient to use the representation of the twist fields in the diagonal basis (see equation (21)) to obtain

$$\mathrm{Tr}\rho_A^n = \prod_{k=0}^{n-1} \langle \mathcal{T}_{n,k}(z,\bar{z})\tilde{\mathcal{T}}_{n,k}(0,0)\rangle, \tag{32}$$

and these two-point functions are known from bosonization (setting $z = \ell$ and $L = 1$ as scale)

$$\langle \mathcal{T}_{n,k}(\ell)\tilde{\mathcal{T}}_{n,k}(0)\rangle = \left|\frac{2\pi\eta(\mathrm{i}\beta)^3}{\theta_1(\ell|\mathrm{i}\beta)}\right|^{2k^2/n^2} \frac{|\theta_\nu(k\ell/n|\mathrm{i}\beta)|^2}{|\theta_\nu(0|\mathrm{i}\beta)|^2}, \tag{33}$$

where θ_ν and η represent standard elliptic functions, and $\nu = 2, 3, 4$ is the sector of the fermion. This gives a simple and compact answer for any integer n, but the analytic continuation of the second part is complicated because k enters in the argument of the θ functions. For this reason, it is possible to give exact expressions for the entanglement entropy only in the high- and low-temperature expansions (that however give convergent expressions). As an example we report here the high-temperature expansion in the NS sector ($\nu = 3$) from [35] :

$$S_A = \frac{1}{3}\log\left[\frac{\beta}{\pi a}\sinh\frac{\pi\ell}{\beta}\right] + \frac{1}{3}\sum_{m=1}^{\infty}\log\frac{\left(1-\mathrm{e}^{2\pi\frac{\ell}{\beta}}\mathrm{e}^{-2\pi\frac{m}{\beta}}\right)\left(1-\mathrm{e}^{-2\pi\frac{\ell}{\beta}}\mathrm{e}^{-2\pi\frac{m}{\beta}}\right)}{\left(1-\mathrm{e}^{-2\pi\frac{m}{\beta}}\right)^2}$$
$$+ 2\sum_{l=1}^{\infty}\frac{(-1)^l}{l}\cdot\frac{\frac{\pi\ell l}{\beta}\coth\left(\frac{\pi\ell l}{\beta}\right)-1}{\sinh\left(\pi\frac{l}{\beta}\right)}. \tag{34}$$

This formula gives one example of the crossover from equation (31) for $\beta \gg 1$ to equation (30) for $\beta \ll 1$. More details about the derivation and the results for other sectors can be found in [35]. We mention that these issues have been investigated numerically for different spin chains in [36].

3.2. Systems with boundaries

In numerical simulations with DMRG and in real experimental life, physical systems do not obey periodic boundary conditions, but rather have some open boundaries. While in the study of correlation functions of local operators the effect of the boundaries can be reduced by performing measures far from them, the intrinsically global nature of the block entanglement makes it more sensitive to the boundary conditions. This is not a negative feature and can be effectively described by boundary CFT [37, 38].

Let us start by considering a 1D system is a semi-infinite line, say $[0, \infty)$, and the subsystem A is the finite interval $[0, \ell)$. The n-sheeted Riemann surface $\tilde{\mathcal{R}}_{n,1}$ then consists of n copies of the half-plane $x \geqslant 0$, sewn together along $0 \leqslant x < \ell$, $\tau = 0$. Once again, we work initially at zero temperature. It is convenient to use the complex variable $w = \tau + \mathrm{i}x$. The uniformizing transformation is now $z = ((w - \mathrm{i}\ell)/(w + \mathrm{i}\ell))^{1/n}$, which maps the whole Riemann surface to the unit disc $|z| \leqslant 1$. In this geometry, $\langle T(z)\rangle = 0$ by rotational invariance, so that, using (22), we find

$$\langle T(w)\rangle_{\tilde{\mathcal{R}}_{n,1}} = \frac{c}{24}(1-n^{-2})\frac{(2\ell)^2}{(w-\mathrm{i}\ell)^2(w+\mathrm{i}\ell)^2}. \tag{35}$$

Note that in the half-plane, T and $\overline{T}$ are related by analytic continuation: $\overline{T}(\bar{w}) = [T(w)]^*$ [37]. Equation (35) has the same form as $\langle T(w)\mathcal{T}_n(\mathrm{i}\ell)\rangle$, which follows from the Ward identities of boundary CFT [37], with the normalization $\langle \mathcal{T}_n(\mathrm{i}\ell)\rangle = (2\ell)^{-d_n}$.

The analysis then proceeds in analogy with the previous case leading to

$$\mathrm{Tr}\,\rho_A^n = \tilde{c}_n \left(\frac{2\ell}{a}\right)^{(c/12)(n-1/n)} \quad \Rightarrow \quad S_A = \frac{c}{6}\log\frac{2\ell}{a} + \tilde{c}_1'. \tag{36}$$

The constants $\tilde{c}_n$ are in principle different from c_n in the periodic case. The coefficient in front of the logarithm is one-half of the one with periodic boundary conditions. This can be interpreted as the analogue of the area law in 1D. In fact, while with periodic conditions there are two boundary points between A and B, in the present case there is only one.

Once again, this result can be conformally transformed into a number of other cases. At finite temperature β^{-1} we find

$$S_A = \frac{c}{6}\log\left(\frac{\beta}{\pi a}\sinh\frac{2\pi\ell}{\beta}\right) + \tilde{c}_1' = \begin{cases} \dfrac{c}{6}\log\dfrac{2\ell}{a} + \tilde{c}_1' & \ell \ll \beta, \\ \dfrac{\pi c}{3\beta}\ell + \tilde{c}_1' & \ell \gg \beta. \end{cases} \tag{37}$$

In the limit $\ell \gg \beta$ we find the same extensive entropy as before. This allows us to identify [3, 40, 43]

$$\tilde{c}_1' - \frac{c_1'}{2} = \log g, \tag{38}$$

where $\log g$ is the boundary entropy, first discussed by Affleck and Ludwig [39]. g depends only on the boundary CFT and its value is known in the simplest cases. Numerical simulations confirm with high precision this relation [40]. It is worth mentioning that the change in the entanglement entropy of topological quantum Hall fluids (see the Fradkin review in this special issue [41] for details) at a point of constriction is related to the change of the Affleck and Ludwig entropy of the coupled edge states of the fluid at the point contact [42].

For a finite 1D system, of length L, at zero temperature, divided into two pieces of length ℓ and $L-\ell$, we similarly find

$$S_A = \frac{c}{6}\log\left(\frac{2L}{\pi a}\sin\frac{\pi\ell}{L}\right) + \tilde{c}_1'. \tag{39}$$

This last equation is the most appropriate for numerical simulations that are usually performed in finite systems with some boundary conditions at both ends.

3.2.1. Interfaces. We have seen that when a system is translationally invariant the entanglement entropy scales like $S_A = c/3\log\ell$, while in the presence of a boundary, that can be a disconnected chain, it scales like $S_A = c/6\log\ell$. In a condensed matter system like a spin chain, we can modulate a single bond (let say at $x = 0$) from zero to the value in the rest of the chain, going from one extreme to the other. In the presence of such a *defect*, there are mainly three possibilities under the renormalization group.

- The defect is irrelevant: the system flows to the translational invariant Hamiltonian and $S_A = c/3\log\ell$.
- The defect is relevant: the RG flow leads the system to a different fixed point. In particular when non-trivial ones are excluded, it flows to a disconnected system with $S_A = c/6\log\ell$.
- The defect is marginal: the critical properties, and in particular the entanglement entropy are the continuous function of the defect strength.

It has been shown numerically [44] and analytically [45] that in the gapless phase of the XXZ chain with $\Delta \neq 0$, the defect is either relevant or irrelevant, leading always to the well-known behaviours of S_A. More interesting is the case of the XX model [46], when the defect is marginal and for the entanglement entropy one gets

$$S_A = \frac{\sigma(t)}{3} \log \ell, \tag{40}$$

where t is the strength of the defect ($t = 0$ for disconnected chains and $t = 1$ for translational invariant ones), and $\sigma(t)$ is a monotonous increasing function of t with $\sigma(0) = 1/2$ and $\sigma(1) = 1$. A similar behaviour has been found also for more complicated defects in [47].

This phenomenon can be described as an interface between two different CFTs with $c = 1$. In [48] the entanglement entropy of two systems of length L separated by an interface with scattering amplitude s (the analogous of t above) has been calculated:

$$S_A = \sigma(|s|) \log L, \quad \text{with} \quad \sigma(|s|) = \frac{|s|}{2} - \frac{2}{\pi^2} \int_0^\infty u(\sqrt{1 + (|s|/\sinh u)^2} - 1)\, \mathrm{d}u, \tag{41}$$

(the integral can also be written in terms of polylog functions). When there is no interface, i.e. for $s = 1$, $\sigma(1) = 1/3$, as expected. Instead $\sigma(0) = 0$ because the two CFTs decouple. Unfortunately, no result for a subsystem of length $\ell < L$ in the presence of the interface is still available to be compared with the results in the XX chain [46].

Other results for more general defects are known [49], but we remand to the review by Laflorencie *et al* in this issue [50] for an extensive discussion.

3.3. General appearance of logarithmic behaviour

In arbitrary dimensions, the scale invariance (i.e. criticality of the statistical model) together with the translational and rotational (i.e. Lorentz in real time) invariance and locality automatically leads to conformal invariance [34], explaining the very large interest in these theories. However, nature is not always so kind and there are physical systems that are critical, but because of the explicit breaking of translational and/or rotational invariance, are not conformal. It is then natural to ask what is the behaviour of the entanglement entropy in these systems. Srednicki [9] argued that the area law in higher dimensional systems for a gapless model should generally collapse to a $\log \ell$ behaviour in one dimension, and so one would expect the appearance of logarithms even in non-conformal invariant systems. Unfortunately, nowadays there are several examples of the breaking of the area scaling in critical systems (see e.g. [6]), leaving doubts on the earlier argument.

Critical systems showing the breaking of translational or rotational invariance have been largely studied. We give here a few important examples. When translational invariance is broken by quenched disorder, the resulting statistical model can be studied by strong-disorder RG methods and numerically. In all the studied models, it has been shown unambiguously that the entanglement entropy always shows a $\log \ell$ behaviour [51–59] (see the review by Moore and Refael [60] in this issue). Translational invariance can also be broken by taking aperiodic couplings: even in this case a $\log \ell$ behaviour has been found [61, 62]. Non-relativistic dispersion relations like $E = k^2$ also naturally break conformal invariance, by breaking Lorentz. A well-known and physical important example is the ferromagnetic Heisenberg chain, for which the entanglement entropy scales like $S_A = 1/2 \log \ell$ [63, 64]. Another interesting example of this kind can be found in [65].

Often it has been proposed that the scaling of the entanglement entropy as $\log \ell$ can be used to define an effective central charge for non-conformally invariant systems that can share some of the properties of the real central charge (as for example the monotonicity along

renormalization group flow [66]). However, conformal invariance is so powerful that it fixes the scaling of the entanglement entropy, but, as we have seen, it also gives precise predictions for finite size scaling in equation (31) and for the scaling of the Rényi entropies (26). Before arguing about the asymptotic restoration of conformal invariance, all these relations should be carefully checked. For example, the finite size scaling found in [64, 65] is different from equation (31). Also the scaling of the entanglement entropy in the zero temperature mixed state of the XXZ chain at $\Delta = 1/2$ scales logarithmically, but has a finite size form different from equation (31) [32] and cannot be described by CFT. Some excited states in spin chains also display logarithmic behaviour because they can be interpreted as ground states of properly defined conformal Hamiltonian [67]. For random systems with quenched disorder, the finite size scaling form seems to be conformal from numerical simulations, but the Rényi entropies have different scaling in the random singlet phase [60]. We also mention that in several collective models a similar logarithmic behaviour has been found [68], but its origin is different from the one discussed here because of the absence of a spatial structure in these mean field-like models. Their properties are related to those of the particle partitioning reviewed by Haque *et al* in this issue [69].

4. Entanglement of disjoint intervals

When the subsystem A consists of several disjoint intervals, the analysis becomes more complicated. In [3] we provided a result that in general is incorrect. This was based on a uniformizing transformation mapping $\mathcal{R}_{n,N}$ into the complex plane. However, the surface $\mathcal{R}_{n,N}$ has genus $(n-1)(N-1)$ and so for $N \neq 1$ (that is the case we already discussed) cannot be uniformized to the complex plane (at the level of the transformation itself, this has been discussed in detail [70]). The case $n = N = 2$ has the topology of a torus, whose partition function depends on the whole operator content of the theory and not only on the central charge. Consequently the simple formulae of [3] cannot be generally correct. The partition functions on Riemann surfaces with higher genus are even more complicated.

Let us then start our analysis from the case of two intervals given by the surface $\mathcal{R}_{n,2}$. By global conformal invariance the partition function (that is the four-point correlation of twist fields) can be written in the form (in this section we adsorb the normalization Z^n into $Z_{\mathcal{R}_{n,N}}$)

$$\mathrm{Tr}\rho_A^n \equiv Z_{\mathcal{R}_{n,2}} = c_n^2 \left(\frac{|u_1 - u_2||v_1 - v_2|}{|u_1 - v_1||u_2 - v_2||u_1 - v_2||u_2 - v_1|} \right)^{2d_n} \mathcal{F}_n(x) \tag{42}$$

where x is the real four-point ratio,

$$x \equiv \frac{z_{12}\, z_{34}}{z_{13}\, z_{24}} = \frac{(u_1 - v_1)(u_2 - v_2)}{(u_1 - u_2)(v_1 - v_2)}, \tag{43}$$

and d_n is given by equation (25). It can also be written as

$$Z_{\mathcal{R}_{n,2}} = Z^W_{\mathcal{R}_{n,2}} \mathcal{F}_n(x), \tag{44}$$

where $Z^W_{\mathcal{R}_{n,2}}$ is the incorrect result in [3]. We normalized such that $\mathcal{F}_n(0) = 1$ (for $x \to 0$, $Z_{\mathcal{R}_{n,2}}$ is the product of the two two-point functions previously calculated and normalized with c_n). The function $\mathcal{F}_n(x)$ depends explicitly on the full operator content of the theory and must be calculated case by case.

In [71], using old results of CFT on orbifolded space [72, 73], $\mathcal{F}_2(x)$ has been calculated for the Luttinger liquid CFT, that is a free boson compactified on a circle of radius R:

$$\mathcal{F}_2(x) = \frac{\theta_3(\eta\tau)\theta_3(\tau/\eta)}{[\theta_3(\tau)]^2}, \tag{45}$$

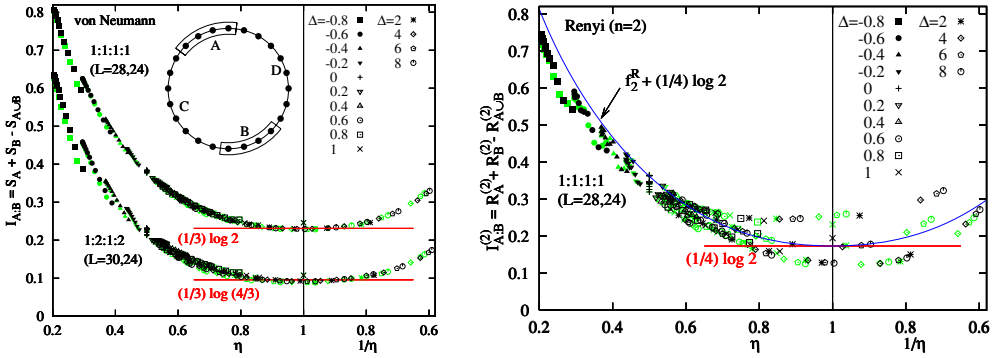

Figure 5. The mutual information for fixed four-point ratio x as a function of η in the gapless phase of the XXZ model. The horizontal lines stand for $Z^W_{\mathcal{R}_{n,2}}$ of [3]. Left: mutual information of the von Neumann entropy. Right: mutual information of the Rényi entropy for $n = 2$, compared with the compactified boson prediction equation (45). Reprinted with permission from [71]. Copyright 2009 by the American Physical Society.

where τ is pure-imaginary, and is related to x via $x = [\theta_2(\tau)/\theta_3(\tau)]^4$. θ_ν are Jacobi theta functions. η is proportional to the square of the compactification radius R (while the definition of R usually depends on the normalization of the action, η is the same throughout the literature, that is why we prefer to write everything only in terms of η that usually is written as $\eta = 1/(2K)$ in Luttinger liquid notation).

In order to check this prediction and the failure of $Z^W_{\mathcal{R}_{n,2}}$, in [71] the entanglement of the XXZ chain for generic values of the anisotropy Δ and magnetic field always in the gapless phase has been calculated by direct diagonalization for systems up to 30 spins. In the absence of the magnetic field, η is related to the anisotropy by $\eta = 1 - (\arccos \Delta)/\pi$, while for non-zero h_z a closed formula for η does not exist and must be calculated numerically as explained in [71]. The main results coming from the exact diagonalization are reported in figure 5 in terms of the Rényi mutual information

$$I^{(n)}_{A_1:A_2} = S^{(n)}_{A_1} + S^{(n)}_{A_2} - S^{(n)}_{A_1\cup A_2}, \tag{46}$$

where A_1 and A_2 are the two intervals composing $A = A_1 \cup A_2$. In figure 5 the mutual information for $n = 1, 2$ is reported. The η dependence in both the cases is evident, and the good collapse of the data shows the correctness of the scaling in equation (42). (In $I^{(2)}_{A_1:A_2}$ the collapse is worst due to the oscillating corrections to the scaling of the Rényi entropies, known already for the single interval [33].) In the right panel of figure 5, the comparison of the numerical results with the prediction (45) is reported. The agreement is satisfactory, considering the small subsystem sizes and the strong oscillations. The results for $I^{(1)}_{A_1:A_2}$ in the left panel of figure 5 are more stable because of the absence of oscillations. These are then more suitable for the comparison with an analytic calculation.

In [74] (in collaboration with E Tonni), we managed to calculate $\mathcal{F}_n(x)$ for generic integral $n \geqslant 1$. The result reads

$$\mathcal{F}_n(x) = \frac{\Theta(0|\eta\Gamma)\,\Theta(0|\Gamma/\eta)}{\Theta(0|\Gamma)^2}, \tag{47}$$

where Γ is an $(n-1)\times(n-1)$ matrix with elements

$$\Gamma_{rs} = \frac{2\mathrm{i}}{n}\sum_{k=1}^{n-1} \sin\left(\pi\frac{k}{n}\right)\beta_{k/n}\cos\left[2\pi\frac{k}{n}(r-s)\right], \tag{48}$$

and

$$\beta_y = \frac{F_y(1-x)}{F_y(x)}, \qquad F_y(x) \equiv_2 F_1(y, 1-y; 1; x). \tag{49}$$

η is exactly the same as above, while Θ is the Riemann–Siegel theta function

$$\Theta(z|\Gamma) \equiv \sum_{m \in \mathbf{Z}^{n-1}} \exp[\,\mathrm{i}\pi\, m \cdot \Gamma \cdot m + 2\pi \mathrm{i}\, m \cdot z], \tag{50}$$

that for $n-1=1$ reduces to the Jacobi θ_3 ($\tau = \mathrm{i}\beta_{1/2}$), reproducing equation (45).

Unfortunately, we have been not yet able to continue analytically this result to real n for generic η and so obtain the entanglement entropy to compare with the left panel of figure 5 from [71].

Some interesting properties can be readily deduced from equation (47).

- For any n, it is symmetric under the exchange $\eta \leftrightarrow 1/\eta$, generalizing the result for $n=2$ in equation (45).
- For $\eta = 1$ the result $Z^W_{\mathcal{R}_{n,2}}$ is correct, i.e. $\mathcal{F}_n(x) = 1$.
- It is symmetric under the exchange $x \leftrightarrow 1-x$ (crossing symmetry). This the scaling limit of $S_A = S_B$ for finite systems [71].

These three important properties carry over to the analytic continuation and so must be true for the von Neumann entropy at $n=1$. These findings then explain the numerical results of [71] (in the left panel of figure 5 the symmetry $\eta \leftrightarrow 1/\eta$ and $\mathcal{F}_1'(x) = 1$ are evident).

More details and other interesting properties can be found in [74]. We discuss here the so-called uncompactified limit for $\eta \gg 1$ or by symmetry $\eta \ll 1$. In this case we have [74] for $\eta \ll 1$,

$$\mathcal{F}_n(x) = \frac{\eta^{-(n-1)/2}}{\left[\prod_{k=1}^{n-1} F_{k/n}(x) F_{k/n}(1-x)\right]^{1/2}} \equiv \frac{\eta^{-(n-1)/2}}{[D_n(x) D_n(1-x)]^{1/2}}, \tag{51}$$

where the function $D_n(x) = \prod_{k=1}^{n-1} F_{k/n}(x)$ has been analytically continued in [74]. Then the prediction

$$I^{(1)}_{A_1:A_2}(\eta \ll 1) - I^{(1),W}_{A_1:A_2} \simeq -\frac{1}{2}\ln\eta + \frac{D_1'(x) + D_1'(1-x)}{2}, \tag{52}$$

perfectly agrees with the numerical results in figure 5 (from [71]) for $\eta \leqslant 0.4$ (again in the previous equation $I^{(1),W}_{A_1:A_2}$ is the result of [3]). Also the regime $x \ll 1$ can be studied analytically [74].

A few comments are now in order. In [16, 75, 76], the entanglement entropy for two disjoint intervals has been calculated for a free Dirac fermion, that corresponds to a compactified boson with $\eta = 1/2$ [34]. However, it has been found that the entanglement entropy is given by $Z^W_{\mathcal{R}_{n,2}}$, in contrast with the numerical calculations in [71] and the analytic one in [74]. The details of this apparent disagreement are still not completely understood, but they should be traced back to the different boundary conditions that result from constructing the reduced density matrix for spin or fermion variables. Another calculation in agreement with $Z^W_{\mathcal{R}_{n,2}}$ can be found in [77]. For the Ising model numerical computations [78] also show a good agreement with $Z^W_{\mathcal{R}_{n,2}}$. Also in this case, it is likely that the deviations from $Z^W_{\mathcal{R}_{n,2}}$ should be attributed to the choice of the variables used in constructing the reduced density matrix. (In fact, calculations in the spin variables [79] show numerically and analytically that $Z^W_{\mathcal{R}_{n,2}}$ is not correct.) Finally, holographic calculations in AdS/CFT correspondence [80, 81], considering the classical limit in the gravity sector, also found $Z^W_{R_{n,2}}$. It would be interesting to understand

how the correct result might arise from taking into account the quantum effects on the gravity side (for details see the review of Nishioka *et al* in this issue [82]).

For general $N > 2$, there are still no firm results in the literature. By global conformal invariance one can deduce

$$\mathrm{Tr}\,\rho_A^n = c_n^N \left(\frac{\prod_{j<k}(u_k - u_j)(v_k - v_j)}{\prod_{j,k}(v_k - u_j)} \right)^{(c/6)(n-1/n)} \mathcal{F}_{n,N}(\{x\}). \tag{53}$$

For $\mathcal{F}_{n,N}(\{x\}) = 1$ this is the incorrect result of [3] (note a typo in the denominator). $\{x\}$ stands for the collection of $2N - 3$ independent ratios that can be built with $2N$ points. Some old results from CFT on orbifold in [73, 83] could be useful to calculate $\mathcal{F}_{n,N}(\{x\})$ for a compactified boson. We also mention that in 2D systems with conformal invariant wavefunction (reviewed in [41] in this volume), the entanglement entropy of a single region displays an addictive universal term depending on η [84].

Finally, it is worth recalling that in the case of more intervals, the entanglement entropy measures only the entanglement of the intervals with the rest of the system. It is *not* a measure of the entanglement of one interval with respect to the others, that instead requires the introduction of more complicated quantities because $A_1 \cup A_2$ is in a mixed state (see e.g. [85] for a discussion of this and examples).

5. Entanglement entropy in non-critical (1+1)-dimensional models

When a one-dimensional statistical model has a gap (i.e. the underlying quantum field theory is massive) the entanglement entropy saturates to a finite value [2]. This is an analogue of the area law in one dimension, because the area is only a number that does not increase with subsystem size, in contrast to higher dimensions. Generally, this value is very complicated to be calculated and it is known only in very simple cases. However, when a system is close to a *conformal* quantum critical point, that is when the gap Δ is small (or the correlation length $\xi \propto \Delta^{-1}$ is large), it is possible to derive a very general scaling form [3], that can be used also as an operative definition of the correlation length. Hastings [86] (see also [87]) provided a rigorous proof of the area law for one-dimensional systems with a generic local Hamiltonian, not necessarily close to a conformal critical point.

We consider an infinite non-critical model in 1+1 dimensions, in the scaling limit where the lattice spacing $a \to 0$ with the correlation length (inverse mass) fixed. This corresponds to a massive relativistic QFT. We first consider the case when the subset A is the negative real axis, so that the appropriate Riemann surface has branch points of order n at 0 and infinity. However, for the non-critical case, the branch point at infinity is unimportant: we should arrive at the same expression by considering a finite system whose length L is much greater than ξ.

Our argument parallels that of Zamolodchikov [66] for the proof of his famous c-theorem. Let us consider the expectation value of the stress tensor $T_{\mu\nu}$ of a massive Euclidean QFT on such a Riemann surface. In complex coordinates, there are three non-zero components: $T \equiv T_{zz}$, $\overline{T} \equiv T_{\bar{z}\bar{z}}$ and the trace $\Theta = 4T_{z\bar{z}} = 4T_{\bar{z}z}$. These are related by the conservation equations

$$\partial_{\bar{z}} T + \tfrac{1}{4}\partial_z \Theta = 0 \qquad \text{and} \qquad \partial_z \overline{T} + \tfrac{1}{4}\partial_{\bar{z}}\Theta = 0. \tag{54}$$

Consider the expectation values of these components. In the single-sheeted geometry, $\langle T \rangle$ and $\langle \overline{T} \rangle$ both vanish, but $\langle \Theta \rangle$ is constant and non-vanishing: it measures the explicit breaking of scale invariance in the non-critical system. In the n-sheeted geometry, however, they all

acquire a non-trivial spatial dependence. By rotational invariance about the origin, they have the form

$$\langle T(z,\bar{z})\rangle = F_n(z\bar{z})/z^2, \tag{55}$$

$$\langle \Theta(z,\bar{z})\rangle - \langle\Theta\rangle_1 = G_n(z\bar{z})/(z\bar{z}), \tag{56}$$

$$\langle \overline{T}(z,\bar{z})\rangle = F_n(z\bar{z})/\bar{z}^2. \tag{57}$$

From the conservation conditions (54) we have

$$(z\bar{z})\big(F_n' + \tfrac{1}{4}G_n'\big) = \tfrac{1}{4}G_n. \tag{58}$$

Now we expect that F_n and G_n both approach zero exponentially fast for $|z| \gg \xi$, while in the opposite limit, on distance scales $\ll \xi$, they approach the CFT values $F_n \to (c/24)(1-n^{-2})$, $G_n \to 0$.

We define an effective C-function

$$C_n(R^2) \equiv \left(F_n(R^2) + \frac{1}{4}G_n(R^2)\right) \quad \Rightarrow \quad R^2\frac{\partial}{\partial(R^2)}C_n(R^2) = \frac{1}{4}G_n(R^2) \tag{59}$$

whose integral, assuming that theory is trivial in the infrared (if the RG flow is towards a non-trivial theory, c should be replaced by $c_{UV} - c_{IR}$), gives

$$\int_0^\infty \frac{G_n(R^2)}{R^2}\,\mathrm{d}(R^2) = -\frac{c}{6}\left(1-\frac{1}{n^2}\right), \tag{60}$$

or equivalently

$$\int \left(\langle\Theta\rangle_n - \langle\Theta\rangle_1\right)\mathrm{d}^2R = -\pi n\frac{c}{6}\left(1-\frac{1}{n^2}\right), \tag{61}$$

where the integral is over the whole of the n-sheeted surface. Now this integral (multiplied by a factor $1/2\pi$ corresponding to the conventional normalization of the stress tensor) measures the response of the free energy $-\log Z$ to a scale transformation, i.e. to a change in the mass m, since this is the only dimensionful parameter of the renormalized theory. Thus, the left-hand side is equal to

$$-(2\pi)\,m\frac{\partial}{\partial m}[\log Z_n - n\log Z], \tag{62}$$

giving finally

$$\frac{Z_n}{Z^n} = c_n(ma)^{(c/12)(n-1/n)}, \tag{63}$$

where c_n is a constant (with however $c_1 = 1$), and we have inserted a power of a, corresponding to the renormalization constant $\mathcal{Z}$ discussed earlier, to make the result dimensionless. Differentiating at $n = 1$, we find

$$S_A = -\frac{c}{6}\log(ma) = \frac{c}{6}\log\frac{\xi}{a}, \tag{64}$$

where ξ is the correlation length. We re-emphasize that this result was obtained only for the scaling limit $\xi \gg a$.

So far we have considered the simplest geometry in the which set A and its complement B are semi-infinite intervals. The more general case, when A is a union of disjoint intervals, is more difficult in the massive case. However, it is still true that the entropy can be expressed in terms of the derivative at $n = 1$ of correlators of twist operators $\mathcal{T}, \tilde{\mathcal{T}}$. The above calculation can be thought of in terms of the one-point function $\langle\mathcal{T}_n\rangle$. In any quantum field theory a more general correlator $\langle\prod_{i=1}^k \Phi(w_i)\rangle$, with $\Phi = \mathcal{T}_n$ or $\tilde{\mathcal{T}}_n$, should obey cluster decomposition: that

is, for separations $|w_i - w_j|$ all $\gg \xi$, it should approach $\langle \mathcal{T}_n \rangle^k$. This suggests that, in this limit, the entropy should behave as

$$S_A = \mathcal{A}\frac{c}{6}\log\frac{\xi}{a}, \tag{65}$$

where $\mathcal{A} = k$ is the number of boundary points between A and its complement. This would be the 1D version of the area law. When the interval lengths are of the order of ξ, we expect to see a complicated but universal scaling form for the crossover.

This scaling has been confirmed in several cases with $\mathcal{A} = 1$ or 2 (see e.g. [3, 23, 24, 88–93], but this list is far from being exhaustive). The corrections to this formula for $\ell \ll \xi$ are also universal [12, 94–96] and are discussed in detail in the review by Castro-Alvaredo and Doyon [97] in this issue.

6. Entanglement spectrum

The knowledge of the scaling form for $\mathrm{Tr}\rho_A^n$ as in equations (26,31,36,63) gives more information about the reduced density matrix than the entanglement entropy. We have seen that in many cases it scales like

$$R_n \equiv \mathrm{Tr}\,\rho_A^n = c_n\,\mathrm{e}^{-b(n-1/n)}, \tag{66}$$

with $b > 0$ only depending on the main features of the set A, on the characteristic length of the system L_{eff} (i.e. ℓ, ξ, $L\sin\pi\ell/L\ldots$) and on the central charge. This suggests that many properties of the reduced density matrix are very universal and do not depend on the details of the theory. For example, the scaling of the largest eigenvalues $\lambda_{\max}$ of ρ_A is obtained by taking the limit for $n \to \infty$ [98]: $S_A^{(\infty)} = -\ln\lambda_{\max} = S_A/2$ defines the so-called 'single-copy entanglement' [99] and gives another measure of the entanglement content of an extended system. This peculiar scaling led to the conclusion that 'half the entanglement in critical systems is distillable from a single specimen' [100].

This result is, however, only the tip of a lot of information about the reduced density matrix obtainable from equation (66). This information is encoded in the full spectrum of the reduced density matrix, which has been called 'entanglement spectrum' for short [101] and has been derived in [102] for 1D systems from equation (66).

In order to characterize the entanglement spectrum, let us define the distribution of eigenvalues $P(\lambda) = \sum_i \delta(\lambda - \lambda_i)$. If we ignore the n dependence of the coefficient c_n (that however is expected only to give corrections the leading behaviour), it is easy to compute the entanglement spectrum by inverse Laplace transforming R_n, obtaining [102]

$$P(\lambda) = \delta(\lambda_{\max} - \lambda) + \frac{b\theta(\lambda_{\max} - \lambda)}{\lambda\sqrt{b\ln(\lambda_{\max}/\lambda)}} I_1(2\sqrt{b\ln(\lambda_{\max}/\lambda)}), \tag{67}$$

where $I_k(x)$ stands for the modified Bessel function of the first kind. Amazingly, $P(\lambda)$ depends only on $\lambda_{\max}$ (we recall $b = -\ln\lambda_{\max}$) and not on any other detail of the theory. For some integrable gapped systems $P(\lambda \ll 1)$ was previously derived [103].

Let us discuss now the main properties of $P(\lambda)$.

- *The mean number of eigenvalues* larger than a given λ is

$$n(\lambda) = \int_{\lambda}^{\lambda_{\max}} \mathrm{d}\lambda\, P(\lambda) = I_0(2\sqrt{b \ln(\lambda_{\max}/\lambda)}). \tag{68}$$

  Note that for $\lambda \to 0$, $n(\lambda)$ diverges, as it should, because in the continuum the number of eigenvalues is infinite. In the lattice models, this can be regularized by the finite number of degrees of freedom.
- *The normalization* $\sum \lambda_i = 1$ corresponds to $\int \lambda P(\lambda)\, \mathrm{d}\lambda = 1$.
- *The entanglement entropy* is given by

$$S = -\int_0^{\lambda_{\max}} \lambda \ln \lambda P(\lambda)\, \mathrm{d}\lambda = -2 \ln \lambda_{\max}, \tag{69}$$

  reproducing the result that the single copy entanglement equals one-half of the entanglement entropy.
- *Majorization* is a relation between two probability distributions $\lambda \equiv \{\lambda_i\}$ and $\mu \equiv \{\mu_i\}$ whose elements are ordered $\lambda_1 > \lambda_2 \cdots > \lambda_N$ (and similarly for μ): it is said that λ majorizes μ if $\sum_{i=1}^{M} \lambda_i \geqslant \sum_{i=1}^{M} \mu_i$ for any $M = 1, \ldots, N$ and $\sum_{i=1}^{N} \lambda_i = \sum_{i=1}^{N} \mu_i = 1$. It has been argued, observed numerically and in some instances proven analytically, that with increasing L_{eff} the resulting distribution of eigenvalues is majorized by the ones at smaller scaling lengths [40, 104]. Majorization follows easily from equation (67):

$$s(M) \equiv \sum_{i=1}^{M} \lambda_i \to \lambda_{\max} \left[1 + \int_0^{I_0^{-1}(M)} \mathrm{d}y\, \mathrm{e}^{-y^2/4b} I_1(y) \right], \tag{70}$$

  at fixed M, is a monotonous function of $\lambda_{\max}$ (that is a monotonous function of L_{eff}). This proves majorization.
- The ratio of the first two eigenvalues (see [102] for details) is

$$\frac{\lambda_2}{\lambda_{\max}} = \mathrm{e}^{k/b} = \mathrm{e}^{-\frac{6k}{c \ln(\ell/a)}}, \tag{71}$$

  where k is a constant and in the second equality we used the result for periodic boundary conditions $b = -\ln \lambda_{\max} = (c/6) \ln(\ell/a)$. This agrees with an old result for the scaling of eigenvalues of the corner transfer matrix [105].

Figure 6 shows an explicit check of the distribution of eigenvalues for the XX model obtained in [102] by using the methods of [106, 107]. It is evident that when the subsystem size ℓ is large enough, the numerical results perfectly agree with equation (70).

The knowledge of the scaling form of the entanglement spectrum has been fundamental in understanding the convergence and the scaling of the algorithms based on matrix product states (MPS) [27], like DMRG. In these algorithms, the maximum amount of entanglement that can be effectively described is limited by the dimension χ of the matrix used to describe the state. The maximum possible entanglement of this state is $S_{\max} = \log \chi$, when all the components have the same weight $1/\chi$. But this maximum entanglement state has nothing to do with the ground state of the local Hamiltonian the algorithm is searching for, because it is described by equation (67). Numerical studies [108, 109], in fact, showed that the entanglement of the MPS approximating the critical ground-state scales like

$$S_A = \frac{c\kappa}{6} \log \chi, \tag{72}$$

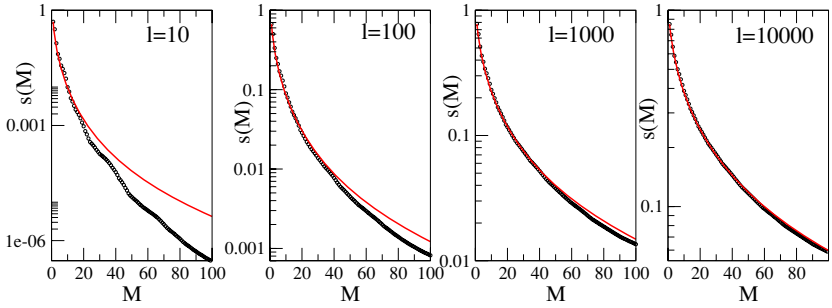

Figure 6. Sum of the first M eigenvalues of the XX model up to $M = 100$: $1 - s(M)$ as a function of M for $\ell = 10, 100, 1000, 10000$ (black dots). The red line is the conformal field theory prediction equation (70), in which $\lambda_{\max}$ has been fixed to the maximum eigenvalue obtained numerically. Numerical data from [102].

(This figure is in colour only in the electronic version)

defining an effective length $\xi_\chi \sim \chi^\kappa$ [108]. κ has been introduced as a new critical exponent of the MPS [108]. Using equation (68), it has been possible to calculate this exponent exactly [109], obtaining

$$\kappa = \frac{6}{c\sqrt{12/c+1}}, \tag{73}$$

and to show that the corrections to equation (72) scale like $1/\log\chi$.

It is worth mentioning that a new numerical algorithm specifically based on the scaling properties of the entanglement in a conformal critical point has been recently proposed by Vidal [110]: the multi-scale entanglement renormalization ansatz (MERA). In MERA, the ground state of an extended quantum system is organized in layers corresponding to different length scales and, at a quantum critical point, each layer equally contributes to the entanglement of a block. This method then allowed us to simulate systems of remarkably large sizes with a relatively little numerical effort. In particular, since the method is explicitly designed for scale invariant systems, some deep connections with CFT have been revealed [111].

7. Entanglement entropy after a quantum quench

The experimental realization of cold atomic systems with a high degree of tunability of Hamiltonian parameters, and the ability to evolve in time with negligible dissipation, is motivating an intensive study of extended quantum systems out of equilibrium. New numerical algorithms have been developed to describe the time evolution of quantum systems effectively (among which adaptive time-dependent DMRG [112], known as tDMRG has been by now the most successful). As for the equilibrium counterpart, the amount of entanglement of the time-dependent state governs the effectiveness of the numerical methods based on MPS. It is then fundamental to have firm bases and expectations for the entanglement growth in non-equilibrium situations. In this case also conformal field theory has been a fundamental tool in understanding very general properties of the time evolution of the entanglement entropy.

The most studied situation (both theoretically and experimentally) is a so-called *quantum quench*. In a quench, an extended quantum system is prepared at time $t = 0$ in a pure state $|\psi_0\rangle$ which is the ground state of some Hamiltonian H_0. For times $t > 0$ the system is allowed

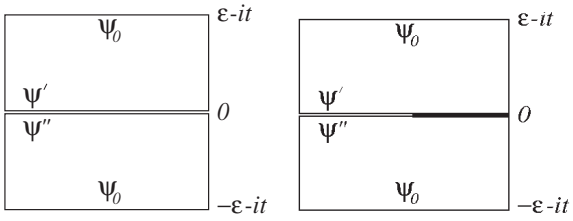

Figure 7. Left: space-imaginary time regions for the density matrix in (75). Right: the reduced density matrix ρ_A is obtained by sewing together along $\tau = 0$ only those parts of the x-axis corresponding to points in B (right part in this plot).

to evolve *unitarily* according to the dynamics given by a different Hamiltonian H, which may be related to H_0 by varying a parameter such as an external field.

Based mainly on the first results from conformal field theory [113, 114] it has been possible to understand that the entanglement entropy grows linearly with time for a so-called global quench (i.e. when the initial state differs globally from the ground state and the excess of energy is extensive), while at most logarithmically for a local one (i.e. when the initial state has only a local difference with the ground state and so a small excess of energy). As a consequence, a local quench can easily be simulated by means of tDMRG, while a global one is harder and the numerics must be limited to relatively small systems sizes. New time-dependent algorithms based explicitly on the possibility of 'storing' more entanglement [115–117] are being developed to have full access to these dynamics.

7.1. Global quench

Suppose we prepare the system in a state $|\psi_0(x)\rangle$ and unitarily evolve it with the Hamiltonian H. The matrix elements of the density matrix at time t are

$$\langle\psi''(x'')|\rho(t)|\psi'(x')\rangle = \langle\psi''(x'')|\mathrm{e}^{-\mathrm{i}tH}|\psi_0(x)\rangle\langle\psi_0(x)|\,\mathrm{e}^{+\mathrm{i}tH}|\psi'(x')\rangle. \tag{74}$$

We modify this time-dependent expectation value as

$$\langle\psi''(x'')|\rho(t)|\psi'(x')\rangle = Z^{-1}\langle\psi''(x'')|\,\mathrm{e}^{-\mathrm{i}tH-\epsilon H}|\psi_0(x)\rangle\langle\psi_0(x)|\,\mathrm{e}^{+\mathrm{i}tH-\epsilon H}|\psi'(x')\rangle, \tag{75}$$

where we have included damping factors $\mathrm{e}^{-\epsilon H}$ in such a way as to make the path integral absolutely convergent. We shall see at the end of the calculation whether it is justified to remove them. The normalization factor $Z = \langle\psi_0(x)|\mathrm{e}^{-2\epsilon H}|\psi_0(x)\rangle$ guarantees that $\mathrm{Tr}\,\rho = 1$.

Each of the factors may be represented by an analytically continued path integral in imaginary time: the first one over fields $\psi(x,\tau)$ which take the boundary values $\psi_0(x)$ on $\tau = -\epsilon - \mathrm{i}t$ and $\psi''(x)$ on $\tau = 0$, and the second with $\psi(z,\tau)$ taking the values $\psi'(x)$ on $\tau = 0$ and $\psi_0(x)$ on $\tau = \epsilon - \mathrm{i}t$. This is illustrated in figure 7. Z is given by the Euclidean path integral over imaginary time 2ϵ, with initial and final conditions both equal to $\psi_0(x)$. This is the same as sewing together the two edges in figure 7 along $\tau = 0$. As before, the reduced density matrix $\rho_A(t)$ is obtained by sewing together along $\tau = 0$ only those parts of the x-axis corresponding to points in B, leaving open slits along A, and $\mathrm{Tr}\,\rho_A^n$ is given by sewing together n copies of this in a cyclic fashion. Thus

$$\mathrm{Tr}\,\rho_A^n = Z_n(A)/Z^n, \tag{76}$$

where Z_n is the path integral on an n-sheeted surface, where the edges of each sheet correspond to imaginary times $-\tau_1$ and τ_2, analytically continued to $\tau_1 = \epsilon + \mathrm{i}t$ and $\tau_2 = \epsilon - \mathrm{i}t$, and

the branch points lie along $\tau = 0$ at the boundaries points between A and B. Finally, the entanglement entropy is given by the derivative of $\mathrm{Tr}\,\rho_A^n$ with respect to n at $n = 1$.

Equation (75) has the form of the equilibrium expectation value in a $(1 + 1)$-dimensional strip geometry with particular boundary conditions. We wish to study this in the limit when t and ℓ are much larger than the microscopic length and time scales, when RG theory can be applied. If H is at (or close to) a quantum critical point, the bulk properties of the critical theory are described by a bulk RG fixed point (or some relevant perturbation thereof). In that case, the boundary conditions flow to one of a number of possible boundary fixed points [118]. Thus, for the purpose of extracting the asymptotic behaviour, we may replace $|\psi_0\rangle$ by the appropriate RG-invariant boundary state $|\psi_0^*\rangle$ to which it flows. The difference may be taken into account, to leading order, by assuming that the RG-invariant boundary conditions are not imposed at $\tau = 0$ and $\tau = 2\epsilon$ but at $\tau = -\tau_0$ and $\tau = 2\epsilon + \tau_0$. In the language of boundary critical behaviour, τ_0 is called the extrapolation length [118]. It characterizes the RG distance of the actual boundary state from the RG-invariant one. It is always necessary because scale-invariant boundary states are not in fact normalizable [38]. It is expected to be of the order of the typical time scale of the dynamics near the ground state of H_0, that is the inverse gap m_0^{-1}. The effect of introducing τ_0 is simply to replace ϵ by $\epsilon + \tau_0$. The limit $\epsilon \to 0^+$ can now safely be taken, so the width of the strip is then taken to be $2\tau_0$.

7.1.1. One interval in the infinite chain. Now we consider the case when H is critical and the field theory is a CFT. First let us consider the case when A is a slit of length ℓ and B is the rest of the real axis. For real τ the strip geometry described above may be obtained from the upper half-plane by the conformal mapping $w = (2\tau_0/\pi)\log z$, with the images of the slits lying along $\arg z = \pi\tau_1/2\tau_0$. The result for Z_n/Z^n in the upper half z-plane, with two branch points follows from equation (42) where half of the points are the images with respect to the real axis. To obtain the result in the strip geometry we transform this two-point correlation function according to equation (29).

After some algebra and continuing to $\tau_1 = \tau_0 + \mathrm{i}t$ (see [113, 119, 120] for detailed calculations), we find for $t, \ell \gg \tau_0$

$$\mathrm{Tr}\,\rho_A^n(t) \simeq c_n \left(\frac{\pi}{2\tau_0}\right)^{2d_n} \left(\frac{\mathrm{e}^{\pi\ell/2\tau_0} + \mathrm{e}^{-\pi\ell/2\tau_0} + 2\cosh(\pi t/\tau_0)}{(\mathrm{e}^{\pi\ell/4\tau_0} - \mathrm{e}^{-\pi\ell/4\tau_0})^2 \cosh^2(\pi t/2\tau_0)}\right)^{d_n} \tilde{\mathcal{F}}_n(x). \tag{77}$$

$\tilde{\mathcal{F}}_n(x)$ is the boundary analogue of $\mathcal{F}_n(x)$ for the four-point function of twist fields in the plane in equation (42). After the conformal mapping and analytically continuing the four-point ratio x becomes large for ℓ/τ_0 and t/τ_0 [119, 120]:

$$x \sim \frac{\mathrm{e}^{\pi t/\tau_0}}{\mathrm{e}^{\pi\ell/2\tau_0} + \mathrm{e}^{\pi t/\tau_0}}. \tag{78}$$

Thus, for $t < \ell/2$ we have $x \sim 0$ and in the opposite case $t > \ell/2$ we have $x \sim 1$. Even if $\tilde{\mathcal{F}}_n(x)$ is generally unknown, we only need its behaviour close to $x \sim 0$ and 1, that are easily deduced from general scaling. Indeed when $x \sim 1$ the two points are deep in the bulk, meaning $\tilde{\mathcal{F}}_n(1) = 1$. Oppositely when $x \ll 1$, the points are close to the boundary and again $\tilde{\mathcal{F}}_n(0) = 1$ (this because $\langle \mathcal{T} \rangle \neq 0$, see [120, 121]). Thus, for the purpose of extracting the asymptotic behaviour, the function $\tilde{\mathcal{F}}_n(x)$ is irrelevant, explaining why the results of [113], obtained within this assumption are correct. Putting everything together, in the case where ℓ/τ_0 and t/τ_0 are large, the moments of the reduced density matrix simplifies to

$$\mathrm{Tr}\,\rho_A^n(t) \simeq c_n(\pi/2\tau_0)^{2d_n} \left(\frac{\mathrm{e}^{\pi\ell/2\tau_0} + \mathrm{e}^{\pi t/\tau_0}}{\mathrm{e}^{\pi\ell/2\tau_0} \cdot \mathrm{e}^{\pi t/\tau_0}}\right)^{d_n}. \tag{79}$$

Differentiating wrt n to get the entropy

$$S_A(t) \simeq -\frac{c}{3}\log\tau_0 + \begin{cases} \dfrac{\pi c t}{6\tau_0} & t < \ell/2, \\ \dfrac{\pi c \ell}{12\tau_0} & t > \ell/2, \end{cases} \tag{80}$$

that is $S_A(t)$ increases linearly until it saturates at $t = \ell/2$. The sharp cusp in this asymptotic result is rounded over a region $|t - \ell/2| \sim \tau_0$. As a difference with [113], following [122], we have added explicitly the subleading constant term $\log\tau_0$ confirming that τ_0 is connected to the inverse mass gap in the initial state.

The result of the entanglement entropy for large time is the same of a mixed state at inverse large finite temperature $\beta_{\rm eff} = 4\tau_0$ (see equation (30)). The physical interpretation of this important effect is that any finite subsystem A reaches a quasi-stationary thermal state, in which the infinite remaining part of the system B act as a thermal bath. It has been shown that, within CFT, this effective temperature is the same for any observable [120] and so can be properly defined. The possibility of defining a Gibbs-like asymptotic state for a general Hamiltonian governing the time evolution (i.e. beyond the CFT case) is a subject of an intensive current activity that would require its own review and that will not be considered at all here.

These results for translationally invariant states have been generalized to inhomogeneous quantum quenches with sharp [123] and smooth [122] initial states.

7.1.2. Physical interpretation. The qualitative, and many of the quantitative, features of $S_A(t)$ found above may be understood physically as follows [113]. The initial state $|\psi_0\rangle$ has a very high energy relative to the ground state of the Hamiltonian H which governs the subsequent time evolution, and therefore acts as a source of quasi-particle excitations. Particles emitted from different points (further apart than the correlation length in the initial state $\propto \tau_0$) are incoherent, but pairs of particles moving to the left or right from a given point are highly entangled. We suppose that the cross-section for producing such a pair of particles of momenta (p', p'') is $f(p', p'')$, and that, once they separate, they move classically. This will of course depend on H and the state $|\psi_0\rangle$, and in principle is calculable, but we made no strong assumptions on its form. If the quasi-particle dispersion relation is $E = E_p$, the classical velocity is $v_p = \mathrm{d}E_p/\mathrm{d}p$. We assume that there is a maximum allowed speed which is taken to be 1, that is $|v_p| \leqslant 1$. A quasi-particle of momentum p produced at x is therefore at $x + v_p t$ at time t, ignoring scattering effects.

Now consider these quasi-particles as they reach either A or B at time t. The field at some point $x' \in A$ will be entangled with that at a point $x'' \in B$ if a pair of entangled particles emitted from a point x arrives simultaneously at x' and x'' (see figure 8). The entanglement entropy between x' and x'' is proportional to the length of the interval in x for which this can be satisfied. Thus, the total entanglement entropy is

$$S_A(t) \approx \int_{x'\in A} \mathrm{d}x' \int_{x''\in B} \mathrm{d}x'' \int_{-\infty}^{\infty} \mathrm{d}x \int f(p', p'')\,\mathrm{d}p'\,\mathrm{d}p''\delta(x' - x - v_{p'}t)\delta(x'' - x - v_{p''}t). \tag{81}$$

Now specialize to the case where A is an interval of length ℓ. The total entanglement is twice that between A and the real axis to the right of A, which corresponds to taking $p' < 0$, $p'' > 0$ in the above. The integrations over the coordinates then give $\max\big((v_{-p'} + v_{p''})t, \ell\big)$,

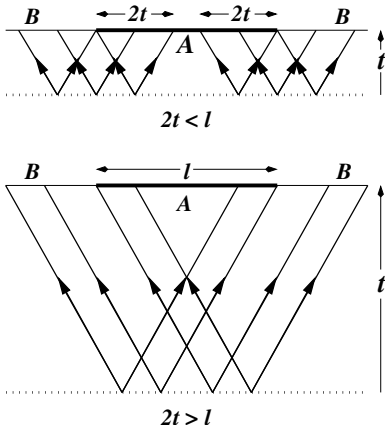

Figure 8. Spacetime picture illustrating how the entanglement between an interval A and the rest of the system, due to oppositely moving coherent quasi-particles, grows linearly and then saturates. The case where the particles move only along the light cones is shown here for clarity. Reprinted with permission from [113].

so that

$$S_A(t) \approx 2t \int_{-\infty}^{0} \mathrm{d}p' \int_{0}^{\infty} \mathrm{d}p'' f(p', p'')(v_{-p'} + v_{p''}) H(\ell - (v_{-p'} + v_{p''})t)$$
$$+ 2\ell \int_{-\infty}^{0} \mathrm{d}p' \int_{0}^{\infty} \mathrm{d}p'' f(p', p'') H((v_{-p'} + v_{p''})t - \ell), \tag{82}$$

where $H(x) = 1$ if $x > 0$ and zero otherwise. Now since $|v_p| \leqslant 1$, the second term cannot contribute if $t < t^* = \ell/2$, so that $S_A(t)$ is strictly proportional to t. On the other hand as $t \to \infty$, the first term is negligible (this assumes that v_p does not vanish except at isolated points), and S_A is asymptotically proportional to ℓ, as found earlier.

However, unless $|v| = 1$ everywhere (as is the case for the CFT calculation), S_A is not strictly proportional to ℓ for $t > t^*$. The rate of approach depends on the behaviour of $f(p', p'')$ in the regions where $v_{-p'} + v_{p''} \to 0$. This generally happens at the zone boundary, and, for a non-critical quench, also at $p' = p'' = 0$. The exact form of $f(p', p'')$ has been exactly calculated only for the XY model in a transverse field [124]. The linear increasing followed by (almost) saturation has been checked in several lattice models both analytically and numerically [53, 113, 124–132], but we do not have room here to discuss the several interesting features that emerged, such as power-law behaviour for large time, periodic time oscillations, etc.

It is worth mentioning that Eisler and Peschel [130] built a lattice model with an exactly linear dispersion relation, and the resulting time-dependent entanglement entropy is exactly the one calculated within CFT. It has been also argued that in random spin chains the initial linear growth of the entanglement entropy is replaced by a logarithmic one [133]. This is a consequence of the strong scattering among quasi-particles and seems to agree with numerical simulations [53].

7.1.3. General result for an arbitrary number of intervals. A general result can be also derived in the case when A consists of the union of the N intervals (u_{2j-1}, u_{2j}) where

$1 \leqslant j \leqslant N$ and $u_k < u_{k+1}$. $\mathrm{Tr}\,\rho_A^n$ is given as usual by the ratio Z_n/Z^n which has the form of a correlation function

$$\left\langle \prod_j \mathcal{T}_n(u_{2j-1} + \mathrm{i}\tau_1) \prod_j \tilde{\mathcal{T}}_n(u_{2j} + \mathrm{i}\tau_1) \right\rangle, \tag{83}$$

in a strip of width $2\tau_0$. We only need the asymptotic behaviour of this correlation function for time t and separations $|u_j - u_k|$ much larger than τ_0. Consequently, the complicated function $\mathcal{F}_{n,N}$ in equation (53) can be set to unity as before. After long algebra one arrives to [113]

$$S_A(t) \sim S_A(\infty) + \frac{\pi c}{12\tau_0} \sum_{k,l} (-1)^{k-l-1} \max(u_k - t, u_l + t). \tag{84}$$

If N is finite (or more generally the u_k are bounded) the second term vanishes for sufficiently large t. At shorter times, $S_A(t)$ exhibits piecewise linear behaviour in t with cusps whenever $2t = u_k - u_l$, at which the slope changes by $\pm\pi c/6\tau_0$ according to whether $k-l$ is even or odd. In the case of an infinite number of regular intervals, with $u_k = k\ell$, $k \in \mathrm{Z}$, $S_A(t)$ exhibits a sawtooth behaviour.

This behaviour can be explained in terms of the quasi-particles arguments of the previous subsection, in which particles entering in and exiting from A entangle and disentangle respectively, giving rise to the non-monotonic behaviour.

The same reasoning applies to other situations, such as for example the time evolution in the presence of boundaries (particularly relevant for tDMRG that are always performed with free boundary conditions). In the simplest instance of the entanglement entropy of the segment $[0, \ell]$ with the rest of the system, the quasi-particle argument is easily understood for a perfect reflecting wall at $x = 0$, for which the resulting *effective* length of the block is 2ℓ and the saturation time $t^* = \ell$, the double of periodic case. This is also easily worked out from the conformal mapping $z = \sin(\pi w/2\tau_0)$ [53, 120].

7.2. Local quench

Suppose we physically cut a spin chain at the boundaries between two subsystems A and B, and prepare a state where the individual pieces are in their respective ground states. In this state the two subsystems are unentangled, and its energy differs from that of the ground state by only a finite amount. Let us join up the pieces at time $-t$ and watch the system evolve up to $t = 0$. The procedure for the global quenches does not apply because the initial state is not translational invariant and will not flow under the renormalization group towards a conformally invariant boundary state. We can represent the corresponding density matrix in terms of path integral on a modified world sheet. The physical cut corresponds to having a slit parallel to the (imaginary) time axis, starting from $-\infty$ up to $\tau_1 = -\epsilon - \mathrm{i}\,t$ (the time when the two pieces have been joined), and analogously the other term of the density matrix gives a slit from $\tau_2 = \epsilon - \mathrm{i}\,t$ to $+\infty$, like in equation (75). Again we introduced the regularization factor ϵ. For computational simplicity we will consider the translated geometry with two cuts starting at $\pm\mathrm{i}\epsilon$ and operator inserted at imaginary time τ. This should be considered real during the course of all the computation, and only at the end can be analytically continued to $\mathrm{i}t$. This plane with the two slits is pictorially represented on the left of figure 9 where $\mathrm{i}\tau$ corresponds to z_1. As shown in the same figure, the z-plane is mapped into the half-plane $\mathrm{Re}\,w > 0$ by means of the conformal mapping

$$w = \frac{z}{\epsilon} + \sqrt{\left(\frac{z}{\epsilon}\right)^2 + 1} \qquad \text{with inverse} \qquad z = \epsilon \frac{w^2 - 1}{2w}. \tag{85}$$

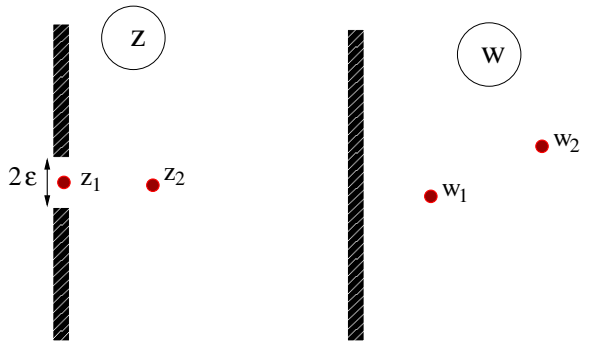

Figure 9. Spacetime region for the density matrix for the local quench (left) mapped to the half-plane (right) by means of equation (85). $z_1 = \mathrm{i}\tau$ and $z_2 = \mathrm{i}\tau + \ell$ during the computation and in the end $\tau \to \mathrm{i}t$. Reprinted with permission from [114].

On the two slits in the z-plane (and so on the imaginary axis in the w one) conformal boundary conditions compatible with the initial state must be imposed.

We consider the time evolution of the entanglement entropy after the local quench of two half chains joined together at the point $r_D = 0$. We consider the four different spatial partitions of the system depicted in figure 10 among which we calculate the entanglement.

7.2.1. Case I: entanglement of the two halves. We start with the more natural division, considering the entanglement entropy between the two parts in which the system was divided before the quench. This is the case when B is the positive real axis and A is the negative real axis. $\mathrm{Tr}\rho_A^n$ transforms like a one-point function that in the w-plane is $[2\mathrm{Re}\ w_1]^{-d_n}$. Thus in the z-plane at the point $z_1 = (0, \mathrm{i}\tau)$ we have

$$\langle \mathcal{T}_n(z_1)\rangle = \tilde{c}_n \left(\left| \frac{\mathrm{d}w}{\mathrm{d}z} \right|_{z_1} \frac{a}{[2\mathrm{Re}\ w_1]} \right)^{d_n} \tag{86}$$

that using $\epsilon w_1 = \mathrm{i}\tau + \sqrt{\epsilon^2 - \tau^2}$ becomes

$$\langle \mathcal{T}_n\rangle = \tilde{c}_n \left(\frac{a\epsilon/2}{\epsilon^2 - \tau^2} \right)^{d_n}. \tag{87}$$

Continuing this result to real time $\tau \to \mathrm{i}t$ we obtain

$$\langle \mathcal{T}_n(t)\rangle = \tilde{c}_n \left(\frac{a\epsilon/2}{\epsilon^2 + t^2} \right)^{d_n}. \tag{88}$$

Using finally the replica trick to find the entanglement entropy we have

$$S_A = -\frac{\partial}{\partial n} \mathrm{Tr}\rho_A^n \Big|_{n=1} = \frac{c}{6} \log \frac{t^2 + \epsilon^2}{a\epsilon/2} + \tilde{c}_1'. \tag{89}$$

For $t \gg \epsilon$ we have

$$S_A(t \gg \epsilon) = \frac{c}{3} \log \frac{t}{a} + k_0, \tag{90}$$

i.e. the leading long time behaviour is only determined by the central charge of the theory in analogy with the ground-state value for a slit. This could result in a quite powerful tool to extract the central charge in time-dependent numerical simulations. The constant k_0 is given by $k_0 = \tilde{c}_1' + (c/6)\log(2a/\epsilon)$.

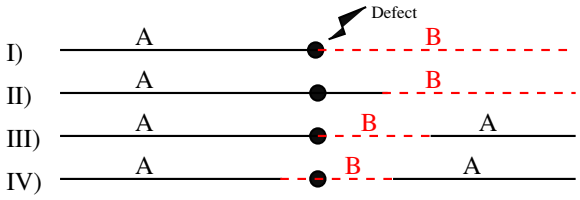

Figure 10. The four different bipartitions of the line we consider in [114]. Reprinted with permission from [114].

The behaviour for short time allows instead to fix the regulator ϵ in terms of the non-universal constant $\tilde{c}_1'$. In fact imposing $S_A(t=0)=0$ we have $\epsilon = a/2\mathrm{e}^{-6\tilde{c}_1'/c}$. Consequently, equation (89) has no free dynamical parameter, in contrast to the case of the global quench.

This short-time $\log t$ behaviour has been observed in different situations with a local defect [134–140].

7.2.2. Case II: decentered defect. Let us now consider the entanglement of the region $r > \ell$ with the rest of the system. In this case $\mathrm{Tr}\rho_A^n$ is equivalent to the one-point function in the plane z at the point $z_2 = \ell + \mathrm{i}\tau$ as in figure 9. Using the conformal mapping (9), analytically continuing and taking $t, \ell \gg \epsilon$ one finally gets [120]

$$S_A = \begin{cases} \dfrac{c}{6}\log\dfrac{2\ell}{a} + \tilde{c}_1' & t < \ell, \\ \dfrac{c}{6}\log\dfrac{t^2-\ell^2}{a^2} + k_0 & t > \ell, \end{cases} \tag{91}$$

with k_0 the same as in equation (90). The interpretation of this result is direct. Indeed at $t = 0$ the joining procedure produces a quasi-particle excitation at $r = 0$ that propagates freely with the corresponding speed of sound v_s that in the CFT normalization is $v_s = 1$. This excitation takes a time $t = \ell$ to arrive at the border between A and B and only at that time will start modifying their entanglement. The following evolution for $t \gg \ell$ is the same as in equation (90).

Also the constant value for $t < \ell$ deserves a comment: it is exactly the value known from CFT for the slit in the half-line equation (36). This is a non-trivial consistency check. Note that a finite ϵ smooths the crossover between the two regimes and makes the entanglement entropy a continuous function of the time.

7.2.3. Cases III and IV: a finite slit. Let us consider again the same physical situation as before, but we now calculate the entanglement entropy of $A = [0, \ell]$ and B the remainder. For $t < 0$ the real negative axis is decoupled from the rest and does not contribute to the entanglement entropy, that is just the one of a slit in half-chain. The entanglement entropy is obtained from the replica trick considering the scaling of a two-point function between the endpoints of the slit, that must be mapped and analytically continued. After lengthy algebra one gets [120]

$$\mathrm{Tr}\rho_A^n = \begin{cases} \tilde{c}_n^2 \left(\dfrac{a^2}{t^2}\dfrac{\ell+t}{\ell-t}\dfrac{\epsilon}{4\ell}\right)^{x_n} \tilde{\mathcal{F}}_n\left(\dfrac{2t}{\ell+t}\right) & t < \ell, \\ \tilde{c}_n^2 \left(\dfrac{a^2}{\ell^2}\right)^{x_n} & t > \ell. \end{cases} \tag{92}$$

Note that compared with [114] we corrected the behaviour for $t < \ell$ with the generally unknown function $\tilde{\mathcal{F}}_n(x)$, the boundary analogue of equation (42), and we used $x = 2t/(\ell+t)$ [114] for the four-point ratio. For $t > \ell$, only $\tilde{\mathcal{F}}_n(1) = 1$ enters and the prediction of [114] remains correct. Using finally the replica trick, we get the entanglement entropy ($\tilde{\mathcal{F}}_1'(x) = -\partial_n \tilde{\mathcal{F}}_n(x)|_{n=1}$)

$$S_A = \begin{cases} \dfrac{c}{3}\ln\dfrac{t}{a} + \dfrac{c}{6}\ln\dfrac{\ell}{\epsilon} + \dfrac{c}{6}\ln 4\dfrac{\ell-t}{\ell+t} + \tilde{\mathcal{F}}_1'\left(\dfrac{2t}{\ell+t}\right) + 2\tilde{c}_1' & t < \ell, \\ \dfrac{c}{3}\ln\dfrac{\ell}{a} + 2\tilde{c}_1' & t > \ell. \end{cases} \tag{93}$$

The crossover time $t^* = \ell$ is again in agreement with the quasi-particles interpretation.

There are several interesting features of this result. For very short time $t \ll \ell$ it reduces to the $\ell = \infty$ case equation (90) as it should. The leading term for $t > \ell$ is just the ground-state value for a slit in an infinite line. However the subleading term is not the same, signaling that for long time the system still remembers something of the initial configuration as a boundary term that is unable to 'dissipate'. Since the extra energy never dissipates under unitary evolution, there is no reason for the constant terms to be the same. According to equation (38) these two constant terms are the same only when $g = 1$, as it is the case for the Ising model with free boundary conditions.

Another interesting feature is the behaviour for $t < \ell$. This is very similar to the form proposed in [135] to fit the numerical data, i.e.

$$S_A = \frac{c_0}{3}\log\ell + \frac{c_1}{3}\log(t/\ell) + \frac{c_2}{3}\log(1-t/\ell) + k'. \tag{94}$$

Only the terms in $t+\ell$ and $\tilde{\mathcal{F}}_1'$ were missing in [135]. However, these behave smoothly for $0 < t < \ell$ and their effect can be well approximate by a constant factor in k'. The results of the fit are $c_0 \simeq 1 + c_2$, $c_1 \simeq 1$ and $c_2 \simeq 1/2$ that are exactly our predictions for $c = 1$.

For the most general case of a slit $A = [\ell_2, \ell_1]$, we remand to the original paper [114]. We stress here that the result for short times (equations (35) and (36) there) are generically incorrect because we assumed $\tilde{\mathcal{F}}_n(x) = 1$, that we learn successively not to be the case. The results for $t > \ell_1$ are instead correct, because in the regime only $\tilde{\mathcal{F}}(1) = 1$ enters and in this case we have

$$S_A(t > \ell_1) = \frac{c}{3}\ln\frac{\ell_1 - \ell_2}{a} + 2\tilde{c}_1', \tag{95}$$

that is the same as for case III. The correct results for $t < \ell_1$ in the various regimes, can be read from equations (48), (50) and (51) in [114] from the general results of the two-point functions of generic primary operators. We mention that we could use non-equilibrium calculations/simulations to determine the unknown function $\tilde{\mathcal{F}}_n(x)$. It is still not clear if this could be effective.

An interesting generalization of the local quantum quench in models with gradients has been provided in [141], where again all the entanglement evolution can be understood in terms of the quasi-particle picture.

7.2.4. Decoupled finite interval. A natural question arising is how the results we just derived change when we introduce more than one defect in the line. It is straightforward to have a path integral for the density matrix: we only need to have pairs of slits from $-\infty$ to $-\mathrm{i}\epsilon$ and from $\mathrm{i}\epsilon$ to $+\mathrm{i}\infty$ resulting in a defect everywhere. However, it becomes prohibitively difficult to treat this case analytically. In order to begin to understand the case when a finite interval is initially decoupled, we consider the case when it lies at the end of a half-line.

So, let us consider a semi-infinite chain in which the A subsystem is the finite segment $(-\ell, 0)$ and the B is the complement $(0, \infty)$ and with the initial defect at $r_D = 0$. The spacetime geometry describing this situation is like the one just considered, with a wall at $-\ell + \mathrm{i}y$ (y real) that represents the boundary condition.

In these circumstances the inverse conformal mapping between the z-plane and the half-plane can be worked out using the Schwarz–Christoffel formula. After lengthy algebra one obtains [114]

$$z(w) = \mathrm{i}\left(\frac{\ell}{\pi}\log(\mathrm{i}w) + b\frac{-\mathrm{i}w - 1}{-\mathrm{i}w + 1}\right), \tag{96}$$

with the parameter b related to ℓ and ϵ in a non-algebraic way. (A slit in the full line is closely related to this transformation, the last piece is replaced by $(w^2 - 1)/(w^2 + 1)$.) Unfortunately, the mapping (96) is not analytically invertible and its exact use is limited to numerical calculations that do not help us, since we need to perform an analytical continuation. However, even if not completely justified, we can take the limit $\ell \gg \epsilon$, before the analytical continuation to real time obtaining [114]

$$w = -\mathrm{i}\exp\left[\frac{\pi}{2\ell}\frac{\mathrm{i}\epsilon}{}\left(\sqrt{z^2/\epsilon^2 + 1} - z/\epsilon\right)\right], \quad \Rightarrow \quad z = \mathrm{i}\frac{\ell}{\pi}\log(\mathrm{i}w) + \mathrm{i}\frac{\epsilon^2}{\ell}\frac{\pi}{4}\frac{1}{\log(\mathrm{i}w)}. \tag{97}$$

This approximation is expected to fail for $t \geqslant \ell$. It is easy to perform the mapping, continuing to real time $\tau \to \mathrm{i}t$, and for $t \gg \epsilon$ we have [114]

$$\langle \mathcal{T}_n(\mathrm{i}\tau)\rangle = \tilde{c}_n\left[\frac{\pi\epsilon}{4\ell}\frac{1}{t\sin(\pi t/2\ell)}\right]^{d_n}. \tag{98}$$

Clearly, this cannot make sense when the argument of the power law becomes negative (i.e. for $t > 2\ell$), signaling the expected failure of equation (97). The time when this approximation fails cannot be understood from this calculation, but only in the comparison with explicit results in real time (or by the exact use of equation (96)). Using the replica trick for the entanglement entropy we obtain

$$S_A = \frac{c}{6}\log\left(\frac{4\ell}{\pi\epsilon}t\sin\frac{\pi t}{2\ell}\right) + \tilde{c}_1'. \tag{99}$$

One is tempted to assume that this result can be correct for $t < \ell$ and that for larger time it saturates as suggested by the quasi-particle interpretation. In the case of an initially decoupled slit of length ℓ in an infinite chain, equation (99) is still valid with the replacements $2\ell \to \ell$ and $c/6 \to c/3$ which follows from a simple analysis [136]. The validity of this equation has been carefully tested for the XX chain in [136], finding very good agreement for all $t < \ell$, confirming the naive expectation. In [47] a more complicated kind of defect has been investigated, and the results always agree with equation (99) when describing a conformal Hamiltonian.

8. Local quench, quantum noise and measuring the entanglement

The entanglement entropy has been revealed to be a useful quantity for a deep theoretical understanding of extended quantum systems, especially in connection with criticality and topological order (see the review by Fradkin in this volume [41]). However, the final check and goal of any theory is the comparison with experiments. The intrinsic non-local nature of the entanglement entropy makes any attempt at an experimental measurement difficult, if not impossible. Some bounds relating S_A to thermodynamic observables have been derived [142], but this is still far from being an operational measure.

However, there is one recent interesting proposal to measure the entanglement entropy out of equilibrium, in the setup of the local quench we have just described [7, 143, 144]. The main idea of Klich and Levitov is to relate the entanglement between two half-chains to the distribution of the electrons passing towards the contact between them. They considered (as we did above) two semi-infinite chains (which are leads in actual experiments) initially disconnected and then at some time t_0 joined together, allowing the passage of electrons (if the leads are two Fermi seas, the quasi-particles of above are real electrons). The transport at this *quantum point contact* is described by the theory of quantum noise. This approach describes the probability distribution of transmitted charge using the generating function $\chi(\lambda) = \sum_{n=-\infty}^{\infty} P_n \, \mathrm{e}^{\mathrm{i}\lambda n}$, where P_n is the probability to transmit n charges in total. The function $\chi(\lambda)$ can be written in terms of cumulants C_m:

$$\log \chi(\lambda) = \sum_{m=1}^{\infty} \frac{(\mathrm{i}\lambda)^m C_m}{m!}. \tag{100}$$

The fundamental point is that the constants C_n are measurable quantities (C_2 is measured in routine experiments, and also C_n up to $n = 5$ have been measured in more difficult experiments).

The main result of [7] is to establish a relation between the cumulants C_n and the entanglement entropy of the two halves

$$S_A = \sum_{m>0} \frac{\alpha_m}{m!} C_m, \qquad \alpha_m = \begin{cases} (2\pi)^m |B_m|, & m \text{ even} \\ 0, & m \text{ odd}, \end{cases} \tag{101}$$

where B_m are Bernoulli numbers. For quantum noise generated in the contact switching on (at t_0) and off (at t_1), the current fluctuations are Gaussian ($C_{m\neq 2} = 0$), with a variance $C_2 = \frac{1}{\pi^2} \log \frac{t_1 - t_0}{\tau}$, where τ is a short time cutoff set by the contact switching rapidity. Combined with equation (101) this gives entropy $S_A \sim (1/3) \log |t_1 - t_0|$. In [7] this has been put in direct relation with the standard formula $S_A = c/3 \log \ell$ ($c = 1$ of free electrons). However, we have seen in the previous section equation (90), that $c/3 \log t$ is a key feature of the local quench that comes from the specific time scale ϵ whose analogous here is τ. In [7] also the reaction of the system to a train of pulses (i.e. periodic switching on and off of the contact) has been considered. When two point contacts are activated at the same time the response should be given by equation (99).

We finally stress that the previous analysis is valid for free electrons, and it is unclear at present how the treatment must be properly modified in general to take into account interactions to describe other universality classes. A first calculation for the Luttinger liquid theory of the quantum Hall point contact showed that the measured noise is always logarithmic, with a prefactor not given by the central charge, but by a filling ν dependent constant [140]:

$$\chi(\lambda) = \exp\left[-\frac{\lambda^2}{2} \frac{\nu}{\pi^2} \log \frac{\Delta t}{\tau} \right], \tag{102}$$

for $\Delta t = t_1 - t_0 \gg \tau$. Furthermore, it has been shown that for the Ising model the noise at a point contact is algebraic instead of logarithmic [140], suggesting that the relation between the full counting statistics and the entanglement could not be structural.

Acknowledgments

We are indebted to several collaborators that contribute to the original works that are partially reviewed here: M Campostrini, O Castro-Alvaredo, B Doyon, M Fagotti, R Fazio, A Lefevre, B Nienhuis, S Sotiriadis, E Tonni. Furthermore, during the last 5 years, we benefited from

very fruitful discussions with many colleagues, among which we particularly thank I Affleck, V Alba, L Amico, J-S Caux, C Castelnovo, J Eisert, F Essler, P Fendley, E Fradkin, J I Latorre, P Le Doussal, J Moore, V Pasquier, R Santachiara, K Schoutens, G Sierra, L Tagliacozzo, E Vicari. This work was supported in part by EPSRC grants EP/D050952/1. PC benefited from a travel grant from ESF (INSTANS activity).

References

[1] Holzhey C, Larsen F and Wilczek F 1994 Geometric and renormalized entropy in conformal field theory *Nucl. Phys.* B **424** 443 (arXiv:hep-th/9403108)

[2] Vidal G, Latorre J I, Rico E and Kitaev A 2003 Entanglement in quantum critical phenomena *Phys. Rev. Lett.* **90** 227902 (arXiv:quant-ph/0211074)
Latorre J I, Rico E and Vidal G 2004 Ground state entanglement in quantum spin chains *Quantum Inf. Comput.* **4** 048 (arXiv:quant-ph/0304098)

[3] Calabrese P and Cardy J 2004 Entanglement entropy and quantum field theory *J. Stat. Mech.* P06002 (arXiv:hep-th/0405152)

[4] Calabrese P, Cardy J and Doyon B (ed) Entanglement entropy in extended systems *J. Phys. A: Math. Theor.* **42** 500301

[5] Amico L, Fazio R, Osterloh A and Vedral V 2008 Entanglement in many-body systems *Rev. Mod. Phys.* **80** 517 (arXiv:quant-ph/0703044)

[6] Eisert J, Cramer M and Plenio M B 2009 Area laws for the entanglement entropy—a review *Rev. Mod. Phys.,* to appear (arXiv:0808.3773)

[7] Klich I and Levitov L 2009 Quantum noise as an entanglement meter *Phys. Rev. Lett.* **102** 100502 (arXiv:0804.1377)

[8] Amico L and Fazio R Entanglement and magnetic order *J. Phys. A: Math. Theor.* **42** 504001

[9] Srednicki M 1993 Entropy and area *Phys. Rev. Lett.* **71** 666 (arXiv:hep-th/9303048)

[10] Wolf M M, Verstraete F, Hastings M B and Cirac J I 2008 Area laws in quantum systems: mutual information and correlations *Phys. Rev. Lett.* **100** 070502 (arXiv:0704.3906)

[11] Calabrese P and Cardy J 2006 Entanglement entropy and quantum field theory: a non-technical introduction *Int. J. Quantum Inf.* **4** 429 (arXiv:quant-ph/0505193)

[12] Cardy J L, Castro-Alvaredo O A and Doyon B 2007 Form factors of branch-point twist fields in quantum integrable models and entanglement entropy *J. Stat. Phys.* **130** 129 (arXiv:0706.3384)

[13] Cardy J 2008 Entanglement entropy in extended quantum systems *Eur. Phys. J.* B **64** 321 (arXiv:0708.2978)

[14] Cardy J and Peschel I 1988 Finite-size dependence of the free energy in two-dimensional critical systems *Nucl. Phys.* B **300** 377

[15] Casini H and Huerta M 2005 Entanglement and alpha entropies for a massive scalar field in two dimensions *J. Stat. Mech.* P05012 (arXiv:cond-mat/0511014)

[16] Casini H, Fosco C D and Huerta M 2005 Entanglement and alpha entropies for a massive Dirac field in two dimensions *J. Stat. Mech.* P05007 (arXiv:cond-mat/0505563)

[17] Casini H and Huerta M 2008 Analytic results on the geometric entropy for free fields *J. Stat. Mech.* P01012 (arXiv:0707.1300)

[18] Casini H and Huerta M 2007 Universal terms for the entanglement entropy in 2+1 dimensions *Nucl. Phys.* B **764** 183 (arXiv:hep-th/0606256)
Casini H, Huerta M and Leitao L 2009 Entanglement entropy for a Dirac fermion in three dimensions: vertex contribution *Nucl. Phys.* B **814** 594 (arXiv:0811.1968)

[19] Casini H and Huerta M 2009 Entanglement entropy in free quantum field theory this special issue arXiv:0905.2562

[20] Belavin A A, Polyakov A M and Zamolodchikov A B 1984 Infinite conformal symmetry in two-dimensional quantum field theory *Nucl. Phys.* B **241** 333

[21] Knizhnik V G 1987 Analytic fields on Riemann surfaces. II *Commun. Math. Phys.* **112** 567

[22] Jin B-Q and Korepin V E 2004 Quantum spin chain, Toeplitz determinants and Fisher–Hartwig conjecture *J. Stat. Phys.* **116** 79 (arXiv:quant-ph/0304108)

[23] Its A R, Jin B-Q and Korepin V E 2005 Entanglement in XY spin chain *J. Phys. A: Math. Gen.* **38** 2975 (arXiv:quant-ph/0409027)

[24] Franchini F, Its A R and Korepin V E 2008 Rényi entropy of the XY spin chain *J. Phys. A: Math. Theor.* **41** 025302 (arXiv:0707.2534)

[25] Igloi F and Juhasz R 2008 Exact relationship between the entanglement entropies of XY and quantum Ising chains *Europhys. Lett.* **81** 57003 (arXiv:0709.3927)
[26] Keating J P and Mezzadri F 2004 Random matrix theory and entanglement in quantum spin chains *Commun. Math. Phys.* **252** 543 (arXiv:quant-ph/0407047)
Keating J P and Mezzadri F 2005 Entanglement in quantum spin chains, symmetry classes of random matrices, and conformal field theory *Phys. Rev. Lett.* **94** 050501 (arXiv:quant-ph/0504179)
[27] Schollwoeck U 2005 The density-matrix renormalization group *Rev. Mod. Phys.* **77** 259 (arXiv:cond-mat/0409292)
Perez-Garcia D, Verstraete F, Wolf M M and Cirac J I 2007 Matrix product state representations *Quantum Inf. Comput.* **7** 401 (arXiv:quant-ph/0608197)
Verstraete F, Murg V and Cirac J I 2008 Matrix product states, projected entangled pair states, and variational renormalization group methods for quantum spin systems *Adv. Phys.* **57** 143 (arXiv:0907.2796)
Verstraete F and Cirac J I 2009 Renormalization and tensor networks in spin chains and lattices this issue
[28] Verstraete F and Cirac J I 2006 Matrix product states represent ground states faithfully *Phys. Rev.* B **73** 094423 (arXiv:cond-mat/0505140)
Schuch N, Wolf M M, Verstraete F and Cirac J I 2008 Entropy scaling and simulability by matrix product states *Phys. Rev. Lett.* **100** 030504 (arXiv:0705.0292)
[29] Korepin V E 2004 Universality of entropy scaling in 1D gap-less models *Phys. Rev. Lett.* **92** 096402 (arXiv:cond-mat/0311056)
[30] Blöte H W J, Cardy J and Nightingale M P 1986 Conformal invariance, the central charge, and universal finite-size amplitudes at criticality *Phys. Rev. Lett.* **56** 742
[31] Affleck I 1986 Universal term in the free energy at a critical point and the conformal anomaly *Phys. Rev. Lett.* **56** 746
[32] Nienhuis B, Campostrini M and Calabrese P 2009 Entanglement, combinatorics and finite-size effects in spin-chains *J. Stat. Mech.* P02063 (arXiv:0808.2741)
[33] Calabrese P, Campostrini M and Nienhuis B *et al* 2009, to appear
[34] Di Francesco P, Mathieu P and Senechal D 1997 *Conformal Field Theory* (New York: Springer)
[35] Azeyanagi T, Nishioka T and Takayanagi T 2008 Near extremal black hole entropy as entanglement entropy via AdS2/CFT1 *Phys. Rev.* D **77** 064005 (arXiv:0710.2956)
[36] Znidaric M, Prosen T and Pizorn I 2008 Complexity of thermal states in quantum spin chains *Phys. Rev.* A **78** 022103 (arXiv:0805.4149)
[37] Cardy J L 1984 Conformal invariance and surface critical behavior *Nucl. Phys.* B **240** 514
[38] Cardy J L 2006 Boundary conformal field theory *Encyclopedia of Mathematical Physics* ed J-P Francoise, G Naber and S Tsun Tsou (Amsterdam: Elsevier) (arXiv:hep-th/0411189)
[39] Affleck I and Ludwig A W W 1991 Universal non-integer 'ground-state degeneracy' in critical quantum systems *Phys. Rev. Lett.* **67** 161
[40] Zhou H-Q, Barthel T, Fjaerestad J O and Schollwoeck U 2006 Entanglement and boundary critical phenomena *Phys. Rev.* A **74** 050305(R) (arXiv:cond-mat/0511732)
[41] Fradkin E 2009 Scaling of entanglement entropy at 2D quantum Lifshitz fixed points and topological fluids this special issue arXiv:0906.1569
[42] Fendley P, Fisher M P A and Nayak C 2007 Topological entanglement entropy from the holographic partition function *J. Stat. Phys.* **126** 1111 (arXiv:cond-mat/0609072)
[43] Laflorencie N, Sorensen E S, Chang M-S and Affleck I 2006 Boundary effects in the critical scaling of entanglement entropy in 1D systems *Phys. Rev. Lett.* **96** 100603 (arXiv:cond-mat/0512475)
[44] Zhao J, Peschel I and Wang X 2006 Critical entanglement of XXZ Heisenberg chains with defects *Phys. Rev.* B **73** 024417 (arXiv:cond-mat/0509338)
Ren J, Zhu S and Hao X 2009 Entanglement entropy in an antiferromagnetic Heisenberg spin chain with boundary impurities *J. Phys. B: At. Mol. Opt. Phys.* **42** 015504
[45] Levine G 2004 Entanglement entropy in a boundary impurity model *Phys. Rev. Lett.* **93** 266402 (arXiv:cond-mat/0408366)
Levine G C and Miller D J 2008 Zero dimensional area law in a gapless fermion system *Phys. Rev.* B **77** 205119 (arXiv:0711.0957)
[46] Peschel I 2005 Entanglement entropy with interface defects *J. Phys. A: Math. Gen.* **38** 4327 (arXiv:cond-mat/0502034)
[47] Igloi F, Szatmari Z and Lin Y-C 2009 Entanglement entropy with localized and extended interface defects *Phys. Rev.* B **80** 024405 (arXiv:0903.3740)
[48] Sakai K and Satoh Y 2008 Entanglement through conformal interfaces *J. High Energy Phys.* JHEP12(2008)001 (arXiv:0809.4548)

[49] Sorensen E S, Chang M-S, Laflorencie N and Affleck I 2007 Impurity entanglement entropy and the Kondo screening cloud *J. Stat. Mech.* L01001 (arXiv:cond-mat/0606705)
Sorensen E S, Chang M-S, Laflorencie N and Affleck I 2007 Quantum impurity entanglement *J. Stat. Mech.* P08003 (arXiv:cond-mat/0703037)
[50] Sorensen E S, Laflorencie N and Affleck I 2009 Entanglement entropy in quantum impurity systems and systems with boundaries this special issue arXiv:0906.1809
[51] Refael G and Moore J E 2004 Entanglement entropy of random quantum critical points in one dimension *Phys. Rev. Lett.* **93** 260602 (arXiv:cond-mat/0406737)
[52] Laflorencie N 2005 Scaling of entanglement entropy in the random singlet phase *Phys. Rev.* B **72** 140408(R) (arXiv:cond-mat/0504446)
[53] De Chiara G, Montangero S, Calabrese P and Fazio R 2006 Entanglement entropy dynamics in Heisenberg chains *J. Stat. Mech.* P03001 (arXiv:cond-mat/0512586)
[54] Santachiara R 2006 Increasing of entanglement entropy from pure to random quantum critical chains *J. Stat. Mech.* L06002 (arXiv:cond-mat/0602527)
[55] Bonesteel N E and Yang K 2007 Infinite-randomness fixed points for chains of non-abelian quasiparticles *Phys. Rev. Lett.* **99** 140405 (arXiv:cond-mat/0612503)
[56] Binosi D, De Chiara G, Montangero S and Recati A 2007 Increasing entanglement through engineered disorder in the random Ising chain *Phys. Rev.* B **76** 140405(R) (arXiv:0707.0266)
[57] Refael G and Moore J E 2007 Entanglement entropy of the random spin-1 Heisenberg chain *Phys. Rev.* B **76** 024419 (arXiv:cond-mat/0703038)
[58] Igloi F and Lin Y-C 2008 Finite-size scaling of the entanglement entropy of the quantum Ising chain with homogeneous, periodically modulated and random couplings *J. Stat. Mech.* P06004 (arXiv:0803.3610)
[59] Fidkowski L, Refael G, Bonesteel N and Moore J 2008 C-theorem violation for effective central charge of infinite-randomness fixed points *Phys. Rev.* B **78** 224204 (arXiv:0807.1123)
[60] Refael G and Moore J E 2009 Criticality and entanglement in random quantum systems this special issue arXiv:0908.1986
[61] Igloi F, Juhasz R and Zimboras Z 2007 Entanglement entropy of aperiodic quantum spin chains *Europhys. Lett.* **79** 37001 (arXiv:cond-mat/0701527)
[62] Juhasz R and Zimboras Z 2007 Entanglement entropy in aperiodic singlet phases *J. Stat. Mech.* P04004 (arXiv:cond-mat/0703527)
[63] Popkov V and Salerno M 2005 Logarithmic divergence of the block entanglement entropy for the ferromagnetic Heisenberg model *Phys. Rev.* A **71** 012301 (arXiv:quant-ph/0404026)
[64] Popkov V, Salerno M and Schuetz G 2005 Entangling power of permutation-invariant quantum states *Phys. Rev.* A **72** 032327 (arXiv:quant-ph/0506209)
[65] Gottesman D and Hastings M B 2009 Entanglement versus gap for one-dimensional spin systems arXiv:0901.1108
[66] Zamolodchikov A B 1986 Irreversibility of the flux of the renormalization group in a 2D field theory *JETP Lett.* **43** 731
Zamolodchikov A B 1986 Irreversibility of the flux of the renormalization group in a 2D field theory *Pisma Zh. Eksp. Teor. Fiz.* **43** 565
[67] Alba V, Fagotti M and Calabrese P 2009 Entanglement entropy of excited states *J. Stat. Mech.* to appear (arXiv:0909.1999)
[68] Latorre J I, Orus R, Rico E and Vidal J 2005 Entanglement entropy in the Lipkin–Meshkov–Glick model *Phys. Rev.* A **71** 064101 (arXiv:cond-mat/0409611)
Barthel T, Dusuel S and Vidal J 2006 Entanglement entropy beyond the free case *Phys. Rev. Lett.* **97** 220402 (arXiv:cond-mat/0606436)
Vidal J, Dusuel S and Barthel T 2007 Entanglement entropy in collective models *J. Stat. Mech.* P01015 (arXiv:cond-mat/0610833)
[69] Haque M, Zozulya O S and Schoutens K 2009 Entanglement between particle partitions in itinerant many-particle states this special issue arXiv:0905.4024
[70] Caraglio M and Gliozzi F 2008 Entanglement entropy and twist fields *J. High Energy Phys.* JHEP11(2008)076 (arXiv:0808.4094)
[71] Furukawa S, Pasquier V and Shiraishi J 2009 Mutual information and compactification radius in a c=1 critical phase in one dimension *Phys. Rev. Lett.* **102** 170602 (arXiv:0809.5113)
[72] Dixon L J, Friedan D, Martinec E J and Shenker S H 1987 The conformal field theory of orbifolds *Nucl. Phys.* B **282** 13
[73] Zamolodchicov Al B 1987 Conformal scalar field on the hyperelliptic curve and critical Ashkin–Teller multipoint correlation functions *Nucl. Phys.* B **285** 481

[74] Calabrese P, Cardy J and Tonni E 2009 Entanglement entropy of two disjoint intervals in conformal field theory *J. Stat. Mech.* to appear (arXiv:0905.2069)
[75] Casini H and Huerta M 2009 Remarks on the entanglement entropy for disconnected regions *J. High Energy Phys.* JHEP03(2009)048 (arXiv:0812.1773)
[76] Casini H and Huerta M 2009 Reduced density matrix and internal dynamics for multicomponent regions *Class. Quantum Grav.* **26** 185005 (arXiv:0903.5284)
[77] Casini H and Huerta M 2004 A finite entanglement entropy and the c-theorem *Phys. Lett.* B **600** 142 (arXiv:hep-th/040511)
[78] Facchi P, Florio G, Invernizzi C and Pascazio S 2008 Entanglement of two blocks of spins in the critical Ising model *Phys. Rev.* A **78** 052302 (arXiv:0808.0600)
[79] Alba V, Tagliacozzo L and Calabrese P 2009 Entanglement entropy of two disjoint blocks in critical Ising models (arXiv:0910.0706)
[80] Ryu S and Takayanagi T 2006 Holographic derivation of entanglement entropy from AdS/CFT *Phys. Rev. Lett.* **96** 181602 (arXiv:hep-th/0603001)
Ryu S and Takayanagi T 2006 Aspects of holographic entanglement entropy *J. High Energy Phys.* JHEP08(2006)045 (arXiv:hep-th/0605073)
[81] Hubeny V E and Rangamani M 2008 Holographic entanglement entropy for disconnected regions *J. High Energy Phys.* JHEP03(2008)006 (arXiv:0711.4118)
[82] Nishioka T, Ryu S and Takayanagi T 2009 Holographic entanglement entropy: an overview arXiv:0905.0932
[83] Bershadsky M and Radul A 1987 Conformal field theories with additional Z_N symmetry *Int. J. Mod. Phys.* A **2** 165
[84] Hsu B, Mulligan M, Fradkin E and Kim E-A 2009 Universal entanglement entropy in 2D conformal quantum critical points *Phys. Rev.* B **79** 115421 (arXiv:0812.0203)
Stephan J-M, Furukawa S, Misguich G and Pasquier V 2009 Shannon and entanglement entropies of one- and two-dimensional critical wave functions arXiv:0906.1153
[85] Wichterich H, Molina-Vilaplana J and Bose S 2009 Scale invariant entanglement at quantum phase transitions *Phys. Rev.* A **80** 010304(R) (arXiv:0811.1285)
Marcovitch S, Retzker A, Plenio M B and Reznik B 2009 Critical and noncritical long range entanglement in the Klein–Gordon field *Phys. Rev.* A **80** 012325 (arXiv:0811.1288)
[86] Hastings M B 2007 An area law for one dimensional quantum systems *J. Stat. Mech.* P08024 (arXiv:0705.2024)
[87] Hastings M B 2007 Entropy and entanglement in quantum ground states *Phys. Rev.* B **76** 035114 (arXiv:cond-mat/0701055)
[88] Peschel I 2004 On the entanglement entropy for a XY spin chain *J. Stat. Mech.* P12005 (arXiv:cond-mat/0410416)
[89] Weston R 2006 The entanglement entropy of solvable lattice models *J. Stat. Mech.* L03002 (arXiv:math-ph/0601038)
[90] Franchini F, Its A R, Jin B-Q and Korepin V E 2007 Ellipses of constant entropy in the XY spin chain *J. Phys. A: Math. Gen.* **40** 8467 (arXiv:quant-ph/0609098)
[91] Its A R, Mezzadri F and Mo M Y 2008 Entanglement entropy in quantum spin chains with finite range interaction *Commun. Math. Phys.* **284** 117 (arXiv:0708.0161)
[92] Ercolessi E, Evangelisti S and Ravanini F 2009 Exact entanglement entropy of the XYZ model and its sine-Gordon limit arXiv:0905.4000
[93] Latorre J I and Riera A 2009 A short review on entanglement in quantum spin systems *J. Phys. A: Math. Theor.* **42** 504002 (arXiv:0906.1499)
[94] Castro-Alvaredo O A and Doyon B 2008 Bi-partite entanglement entropy in integrable models with backscattering *J. Phys. A: Math. Theor.* **41** 275203 (arXiv:0802.4231)
[95] Doyon B 2009 Bi-partite entanglement entropy in massive two-dimensional quantum field theory *Phys. Rev. Lett.* **102** 031602 (arXiv:0803.1999)
[96] Castro-Alvaredo O A and Doyon B 2009 Bi-partite entanglement entropy in massive QFT with a boundary: The Ising model *J. Stat. Phys.* **134** 105 (arXiv:0810.0219)
[97] Castro-Alvaredo O A and Doyon B 2009 Bi-partite entanglement entropy in massive 1+1-dimensional quantum field theories this issue arXiv:0906.2946
[98] Peschel I and Zhao J 2005 On single-copy entanglement *J. Stat. Mech.* P11002 (arXiv:quant-ph/0509002)
[99] Eisert J and Cramer M 2005 Single-copy entanglement in critical spin chains *Phys. Rev.* A **72** 042112 (arXiv:quant-ph/0506250)
[100] Orus R, Latorre J I, Eisert J and Cramer M 2006 Half the entanglement in critical systems is distillable from a single specimen *Phys. Rev.* A **73** 060303 (arXiv:quant-ph/0509023)

[101] Li H and Haldane F D M 2008 Identifying topological order from the 'entanglement spectrum' *Phys. Rev. Lett.* **101** 010504 (arXiv:0805.0332)
[102] Calabrese P and Lefevre A 2008 Entanglement spectrum in one-dimensional systems *Phys. Rev.* A **78** 032329 (arXiv:0806.3059)
[103] Okunishi K, Hieida Y and Akutsuet Y 1999 Universal asymptotic eigenvalue distribution of density matrices and corner transfer matrices in the thermodynamic limit *Phys. Rev.* E **59** R6227
[104] Latorre J I, Lutken C A, Rico E and Vidal G 2005 Fine-grained entanglement loss along renormalization group flows *Phys. Rev.* A **71** 034301 (arXiv:quant-ph/0404120)
Orus R 2005 Entanglement and majorization in (1+1)-dimensional quantum systems *Phys. Rev.* A **71** 052327
Orus R 2006 Entanglement and majorization in (1+1)-dimensional quantum systems *Phys. Rev.* A **73** 019904(E) (arXiv:quant-ph/0501110)
[105] Peschel I and Truong T T 1987 Corner transfer matrices and conformal invariance *Z. Phys.* B **69** 385
[106] Peschel I, Kaulke M and Legeza O 1999 Density-matrix spectra for integrable models *Ann. Phys. (Leipzig)* **8** 153 (arXiv:cond-mat/9810174)
Peschel I and Chung M-C 1999 Density matrices for a chain of oscillators *J. Phys. A: Math. Gen.* **32** 8419 (arXiv:cond-mat/9906224)
Chung M-C and Peschel I 2001 Density-matrix spectra of solvable fermionic systems *Phys. Rev.* B **64** 064412 (arXiv:cond-mat/0103301)
Peschel I 2003 Calculation of reduced density matrices from correlation functions *J. Phys. A: Math. Gen.* **36** L205 (arXiv:cond-mat/0212631)
Peschel I 2004 On the reduced density matrix for a chain of free electrons *J. Stat. Mech.* P06004 (arXiv:cond-mat/0403048)
[107] Peschel I and Eisler V 2009 Reduced density matrices and entanglement entropy in free lattice models arXiv:0906.1663
[108] Tagliacozzo L, de Oliveira T R, Iblisdir S and Latorre J I 2008 Scaling of entanglement support for matrix product states *Phys. Rev.* B **78** 024410 (arXiv:0712.1976)
[109] Pollmann F, Mukerjee S, Turner A and Moore J E 2009 Theory of finite-entanglement scaling at one-dimensional quantum critical points *Phys. Rev. Lett.* **102** 255701 (arXiv:0812.2903)
[110] Vidal G 2007 Entanglement renormalization *Phys. Rev. Lett.* **99** 220405 (arXiv:cond-mat/0512165)
[111] Pfeifer R N C, Evenbly G and Vidal G 2009 Entanglement renormalization, scale invariance, and quantum criticality *Phys. Rev.* A **79** 040301(R) (arXiv:0810.0580)
Giovannetti V, Montangero S and Fazio R 2008 Quantum MERA channels *Phys. Rev. Lett.* **101** 180503 (arXiv:0804.0520)
[112] Daley A J, Kollath C, Schollwoeck U and Vidal G 2004 Time-dependent density-matrix renormalization-group using adaptive effective Hilbert spaces *J. Stat. Mech.* P04005 (arXiv:cond-mat/0403313)
White S R and Feiguin A E 2004 Real time evolution using the density matrix renormalization group *Phys. Rev. Lett.* **93** 076401 (arXiv:cond-mat/0403310)
[113] Calabrese P and Cardy J 2005 Evolution of entanglement entropy in one dimensional systems *J. Stat. Mech.* P04010 (arXiv:cond-mat/0503393)
[114] Calabrese P and Cardy J 2007 Entanglement and correlation functions following a local quench: a conformal field theory approach *J. Stat. Mech.* P10004 (arXiv:0708.3750)
[115] Rizzi M, Montangero S and Vidal G 2008 Simulation of time evolution with multiscale entanglement renormalization ansatz *Phys. Rev.* A **77** 052328 (arXiv:0706.0868)
[116] Hastings M B 2008 Observations outside the light-cone: algorithms for non-equilibrium and thermal states *Phys. Rev.* B **77** 144302 (arXiv:0801.2161)
[117] Banuls M C, Hastings M B, Verstraete F and Cirac J I 2009 Matrix product states for dynamical simulation of infinite chains *Phys. Rev. Lett.* **102** 240603 (arXiv:0904.1926)
[118] Diehl H W 1986 The theory of boundary critical phenomena *Phase Transitions and Critical Phenomena* vol 10 ed C Domb and J L Lebowitz (London: Academic)
Diehl H W 1997 The theory of boundary critical phenomena *Int. J. Mod. Phys.* B **11** 3503 (arXiv:cond-mat/9610143)
[119] Calabrese P and Cardy J 2006 Time-dependence of correlation functions following a quantum quench *Phys. Rev. Lett.* **96** 136801 (arXiv:cond-mat/0601225)
[120] Calabrese P and Cardy J 2007 Quantum quenches in extended systems *J. Stat. Mech.* P06008 (arXiv:0704.1880)
[121] Cardy J and Lewellen D 1991 Bulk and boundary operators in conformal field theory *Phys. Lett.* B **259** 274
[122] Sotoriadis S and Cardy J 2008 Inhomogeneous quantum quenches *J. Stat. Mech.* P11003 (arXiv:0808.0116)

[123] Calabrese P, Hagendorf C and Le Doussal P 2008 Time evolution of 1D gapless models from a domain-wall initial state: SLE continued? *J. Stat. Mech.* P07013 (arXiv:0804.2431)
[124] Fagotti M and Calabrese P 2008 Evolution of entanglement entropy following a quantum quench: analytic results for the XY chain in a transverse magnetic field *Phys. Rev.* A **78** 010306(R) (arXiv:0804.3559)
[125] Eisert J and Osborne T J 2006 General entanglement scaling laws from time evolution *Phys. Rev. Lett.* **97** 150404 (arXiv:quant-ph/0603114)
Bravyi S, Hastings M B and Verstraete F 2006 Lieb–Robinson bounds and the generation of correlations and topological quantum order *Phys. Rev. Lett.* **97** 050401 (arXiv:quant-ph/0603121)
[126] Cincio L, Dziarmaga J, Rams M M and Zurek W H 2007 Entropy of entanglement and correlations induced by a quench: dynamics of a quantum phase transition in the quantum Ising model *Phys. Rev.* A **75** 052321 (arXiv:cond-mat/0701768)
[127] Prosen T and Znidaric M 2007 Is efficiency of classical simulations of quantum dynamics related to integrability? *Phys. Rev.* E **75** 015202 (arXiv:quant-ph/0608057)
[128] Schuch N, Wolf M M, Vollbrecht K G H and Cirac J I 2008 On entropy growth and the hardness of simulating time evolution *New J. Phys.* **10** 033032 (arXiv:0801.2078)
[129] Laeuchli A and Kollath C 2008 Spreading of correlations and entanglement after a quench in the Bose–Hubbard model *J. Stat. Mech.* P05018 (arXiv:0803.2947)
[130] Eisler V and Peschel I 2008 Entanglement in a periodic quench *Ann. Phys. (Berlin)* **17** 410 (arXiv:0803.2655)
[131] Manmana S R, Wessel S, Noack R M and Muramatsu A 2009 Time evolution of correlations in strongly interacting fermions after a quantum quench *Phys. Rev.* B **79** 155104 (arXiv:0812.0561)
[132] Barthel T, Kasztelan C, McCulloch I P and Schollwöck U 2009 Magnetism, coherent many-particle dynamics, and relaxation with ultracold bosons in optical superlattices *Phys. Rev.* A **79** 053627 (arXiv:0809.5141)
[133] Burrell C K and Osborne T J 2007 Bounds on information propagation in disordered quantum spin chains *Phys. Rev. Lett.* **99** 167201 (arXiv:quant-ph/0703209)
[134] Gobert D, Kollath C, Schollwoeck U and Schuetz G 2005 Real-time dynamics in spin-1/2 chains with adaptive time-dependent DMRG *Phys. Rev.* E **71** 036102 (arXiv:cond-mat/0409692)
[135] Eisler V and Peschel I 2007 Evolution of entanglement after a local quench *J. Stat. Mech.* P06005 (arXiv:cond-mat/0703379)
[136] Eisler V, Karevski D, Platini T and Peschel I 2008 Entanglement evolution after connecting finite to infinite quantum chains *J. Stat. Mech.* P01023 (arXiv:0711.0289)
[137] Kleine A, Kollath C, McCulloch I P, Giamarchi T and Schollwoeck U 2008 Excitations in two-component Bose-gases *New J. Phys.* **10** 045025 (arXiv:0712.1448)
[138] Perales A and Vidal G 2008 Entanglement growth and simulation efficiency in one-dimensional quantum lattice systems *Phys. Rev.* A **78** 042337 (arXiv:0711.3676)
[139] Pizorn I and Prosen T 2009 Operator space entanglement entropy in XY spin chains *Phys. Rev.* B **79** 184416 (arXiv:0903.2432)
[140] Hsu B, Grosfeld E and Fradkin E 2009 Quantum noise and entanglement generated by a local quantum quench arXiv:0908.2622
[141] Eisler V, Igloi F and Peschel I 2009 Entanglement in spin chains with gradients *J. Stat. Mech.* P02011 (arXiv:0810.3788)
[142] Klich I, Refael G and Silva A 2006 Towards measuring entanglement entropies in many body systems *Phys. Rev.* A **74** 032306 (arXiv:cond-mat/0603004)
[143] Klich I and Levitov L 2008 Scaling of entanglement entropy and superselection rules arXiv:0812.0006
[144] Klich I and Levitov L 2009 Many-body entanglement: a new application of the full counting statistics *Adv. Theor. Phys.* **1134** 36 (arXiv:0901.3391)